ROTORCRAFT TECHNOLOGY AT BOEING VERTOL: RECENT ADVANCES

John Shaw, Leo Dadone, and Robert Wiesner
Boeing Vertol Company

ABSTRACT

This paper presents an overview of key accomplishments in Boeing Vertol's Independent Research and Development (IR&D) program during the past several years, and a more detailed review of two IR&D projects of particular significance: high speed rotor development and the Model 360 Advanced Technology Helicopter. Areas addressed in the overview are: advanced rotors with reduced noise and vibration, 3-D aerodynamic modeling, flight control and avionics, active control, automated diagnostics and prognostics, composite structures, and drive systems.

OVERVIEW

Key rotorcraft programs currently in progress at Boeing Vertol are the V-22 Osprey tiltrotor (in full scale development), the LHX light helicopter family (in preliminary design), and the Model 360 Advanced Technology Helicopter (in final assembly prior to flight testing). These aircraft are shown in Figure 1.

To support these and other, future rotorcraft developments, Boeing Vertol is conducting an aggressive research program across the entire range of rotorcraft technology, with emphasis in seven areas:

- Advanced rotors with reduced noise and vibration
- 3-D aerodynamic modeling
- Flight control and avionics
- Active control
- Automated diagnostics and prognostics
- Composite structures
- Drive systems

The first five of these areas reflect rapidly advancing computing technology which is applied both in design (math modeling, optimization, computer-aided design) and on the aircraft itself (e.g. fly-by-optics, higher harmonic control, expert systems). The last two areas reflect rapidly advancing materials technology.

The past five years have been marked by major progress in all of these areas. This paper begins with an overview of key accomplishments,

emphasizing the Independent Research and Development (IR&D) program, followed by a more detailed review of two particular IR&D highlights: high speed rotor development and the Model 360 Advanced Technology Helicopter.

ADVANCED ROTORS

Boeing Vertol IR&D on advanced rotors is focused on the development of design methodology for high speed, high performance rotors with low vibration and noise. This involves improving predictive methods for vibration and noise, evaluating low vibration and low noise design approaches, and developing optimization technology. Central to all of these activities have been major breakthroughs in the understanding and modeling of vortex wakes, complemented by comprehensive improvement of the supporting data base using an array of wind tunnel models with better aerodynamic and vibratory load instrumentation than ever before. Many of these advances are described in some detail in a later part of this paper. IR&D programs have been a vital base for current contract R&D programs to develop the airloads and induced velocity program element for the Second Generation Comprehensive Helicopter Analysis System - 2GCHAS (U. S. Army-Ames), to develop and test an advanced bearingless rotor concept in the 40- by 80-ft. wind tunnel (NASA-Ames), and to design and test an Advanced Technology Blade for the XV-15 tilt rotor aircraft (NASA-Ames).

The data base for advanced rotor acoustics was greatly increased in 1986 by testing a dynamically scaled, pressure-instrumented model of the Boeing Vertol Model 360 rotor in the German-Dutch acoustic wind tunnel (DNW). The test installation is shown in Figure 2. The Model 360 data, which shows the benefits of second-generation transonic airfoils and tapered blade tips, will be used in 1987 to validate predictive methology for rotor noise of all types, particularly blade/vortex interaction and shock noise. (Validation is already under way using data from earlier testing of a similar model in the Boeing Vertol wind tunnel under NASA contract, as a part of the National Rotor Noise Research $(NR)^2$ program). Recent improvements have been made in the predictive methology, particularly in the area of thickness noise for tapered blades.

The data base for advanced rotor aerodynamics and vibratory loads was also greatly increased by the Model 360 rotor test in the DNW. This data, extending to almost 200 knots, will be used to validate recently improved high speed rotor loads methodology including new wake models, as well as transonic codes developed by NASA (Dr. I. C. Chang), the U. S. Army (Dr. F. X. Caradonna), and Dr. L. N. Sankar at Georgia Institute of Technology. This work is described in greater detail in later sections of the paper.

Development of optimization technology has focused on the reduction of vibratory hub loads by tailoring blade physical properties. Major reductions of vertical hub loads have been shown analytically; current work involves the inplane hub loads. Recent results are shown in Figure 3.

Vibratory airloads of the tilt rotor configuration were explored recently as a part of the IR&D program by testing a scaled, powered model of the V-22 Osprey in the Boeing Vertol wind tunnel. This provided a data base to validate methodology for the wing-rotor aerodynamic interaction.

3-D AERODYNAMIC MODELING

The Boeing Vertol IR&D program on 3-D aerodynamic modeling addresses the development of predictive methodology in two areas: a) airframe pressure distributions and b) rotor/airframe aerodynamic interactions.

The methodology developed to date for airframe pressure distributions involves potential flow panel methods, primarily PANAIR and VSAERO. These are being applied to cases which involve separated flow, a key element of rotorcraft aerodynamics. While the emphasis in fixed-wing aircraft design is the elimination of separated flow, separation can only be minimized, not eliminated, in V/STOL aircraft. The modeling of separated flow becomes critical in the definition of blunt fuselages and afterbodies. The VSAERO code has been formulated specifically to model separated flows and wakes. Figures 4 and 5 illustrate recent progress in applying and validating this methodology using pressure distributions measured in the wind tunnel. Figure 4 shows test/theory correlation in the prediction of tiltrotor fuselage pressure distributions. Figure 5 shows test/theory correlation in the prediction of wind tunnel mounting system interference effects.

Interactional aerodynamics concerns mutual interference effects between the airframe and the rotor(s), specifically (a) the rotor inflow changes and wake distortion induced by the airframe and (b) the steady and vibratory pressures induced by the blades and rotor wake on fuselage, wings, empennage etc. Preliminary rotor-on-fuselage and fuselage-on-rotor methodology involving non-impinging wakes was developed and validated a number of years ago. Today's V/STOL design requirements make it necessary that flow separation and fully interactive and impinging wakes be introduced in the potential flow models. Major progress has been made in this area in the past several years.

Plans for 1987 call for work with TRANAIR, a transonic panel code developed by Boeing under contract to NASA-Ames, and subsequently with Euler codes developed by NASA-Ames and the U. S. Army.

FLIGHT CONTROL AND AVIONICS

Boeing Vertol has led the industry in the development of advanced flight control systems, having flown the first two demonstration fly-by-wire systems for rotorcraft (TAGS, 1969 and HLH/Model 347, 1972), flown the first demonstration fly-by-optics system for any aircraft (ADOCS, 1985), developed the first production fly-by-wire system for rotorcraft (V-22, 1987), and developed the first all-digital AFCS for rotorcraft which incorporates Large Scale Integrated electronics (the 1750A microchip processor) and higher order language (JOVIAL-73) (Model 360, 1987). As an important part of these programs, Boeing Vertol has led in the development and integration of sidearm control. IR&D has been an important element in developing the technology base for these key advances. The critical thrust has been to simplify the system hardware to achieve high reliability. IR&D has been -- and is being -- used to develop fault-tolerant system architectures, methodology for error-free software, and sidearm controller technology. Optical-hydraulic valves, the least-developed element of fly-by-optics, are also being

evaluated in the IR&D program. Additionally, IR&D is aimed at development of computer-aided control law design methodology and improvement of simulation models, methodology for flight control/structural interaction, and analyses of rotorcraft flight dynamics.

To support the V-22 Osprey, the LHX program, and the R&D programs just described, the Boeing Vertol Flight Simulation Laboratory is being upgraded in major ways. The most important of these are an advanced Evans and Sutherland CT6 Computer Image Generation system with special features appropriate to LHX mission requirements and with capability to fly two aircraft "eyepoints" simultaneously over the same terrain (Figure 6); a dome for projection of computer-generated images over the entire 360° field-of-view; and a six degree of freedom motion base with interchangeable cab capability (initially V-22 or LHX). The expanded simulation facility occupies 25,000 square feet, and is located adjacent to an avionics integration facility. Together, the two facilities allow complete piloted checkout of flight control/avionics hardware and software functions prior to flight. This reduces flight control/avionics flight development cost and increases flight safety through pre-flight piloted simulation of difficult mission profiles and fault conditions. The integrated laboratory is a key element in validating the flight control/avionics software utilized in highly automated next-generation aircraft.

ACTIVE CONTROL

Boeing Vertol has a major IR&D program in active control which is focused primarily on higher harmonic control (HHC) applied to conventional rotor blades through the swashplate. The program has addressed the full range of HHC design issues in depth, using a combination of analysis and wind tunnel testing. This IR&D is unusually comprehensive relative to other HHC programs in the rotorcraft industry: it has addressed both three-and four-bladed rotors, articulated and hingeless rotors, single and tandem configurations, fixed-gain, scheduled-gain, and adaptive controllers, actuator mechanical and servoloop design, and performance improvement as well as vibration reduction. Wind tunnel testing of a scaled CH-47D rotor in 1984 was particularly successful, demonstrating a fully effective, fixed-gain control law over the entire test envelope up to 188 knots (Figure 7) plus precise high frequency actuator control and long-life actuator mechanical design. This testing provides an excellent data base for design of full-scale HHC systems which are both effective and efficient. The results have been utilized in contract R&D work for the U. S. Army - AATD for preliminary design of an HHC system for the UH-60A Black Hawk. Current efforts include evaluation of active control in a variety of new applications.

AUTOMATED DIAGNOSTICS AND PROGNOSTICS

Boeing Vertol's IR&D work in automated diagnostics and prognostics includes the development of several expert systems. The first of these, a system for rotor track and balance of newly built aircraft, was developed in 1986. That system will soon be greatly expanded to form an expert system which diagnoses all types of 1/rev vibration problems on fielded aircraft, under contract to U. S. Army - AATD. The benefits of these systems in reducing

the number of test flights required for track and balance are shown in Figure 8. The same AATD contract has already extended exploratory IR&D work on flight control system diagnostics to a complete expert system for this purpose. Further IR&D projects to develop prognostic systems for transmissions and flight control actuators are now under way. Also under development is an automated NOE navigator, the first element of an automated pilot's associate which will include on-line diagnostics and prognostics.

COMPOSITE STRUCTURES

Boeing Vertol IR&D on composite structures has been focused since 1981 on a major project which has advanced the state of the art in every area of structures technology: the Model 360 Advanced Technology Helicopter. The Model 360 is presently in final assembly and is scheduled to fly in early 1987. This innovative aircraft embodies two major thrusts in composite structures: a) a very significant reduction of airframe weight and cost through wide use of composite honeycomb structure, and b) major extension of the damage/defect tolerance achievable with composites to the dynamic system wherever possible. Accomplishments in these areas are discussed in some detail in a later part of this paper. IR&D has also been used to conduct a research program in conjunction with MIT's Technology Laboratory for Advanced Composites initially to evaluate damage tolerance of graphite composite shear panels and more recently to develop a theoretical model for cumulative fatigue damage in composites.

DRIVE SYSTEMS

IR&D work in drive systems has included the development of 3-D finite element modeling techniques for gears and their supporting bearing systems, evaluation of improved gear steels and advanced housing materials, and evaluation of gear surface coatings to increase transmission efficiency and reduce lubrication requirements. The work on gear modeling, illustrated in Figure 9, is unique and valuable. It has led to the development of a gear rim thickness factor which enables more efficient and reliable design and which has been added to AGMA standards. It has also led to a modification of the AGMA standard for the size factor used in spiral bevel gear design. The work on improved gear steels has led the industry in three areas: application of high-hot-hardness (H^3) steels which greatly increase safety under conditions of marginal lubrication; development of cleaner steels which increase safety under all conditions; and application of fracture mechanics to establish threshhold stress levels for zero crack propagation as a function of material cleanliness. The evaluation of advanced housing materials led to a contract R&D program with U.S. Army - AATD for full-scale evaluation of graphite/polyimide and FP/magnesium metal matrix composite housings. Additionally, Boeing Vertol has just completed R&D under contract to U. S. Army - AATD for development of large transmission technology, through improvements to transmissions designed for the Heavy Lift Helicopter. This program achieved successful operation of the highest power level gear mesh ever built for aircraft application (over 10,000 HP). A further IR&D accomplishment in 1986 is the development of the first integrated all-composite shaft and coupling designed to tolerate high misalignment angles (Figure 10). The extremely light weight and simplicity of this shaft-coupling combination are unique advantages in providing dynamic

stability in applications with next-generation, high-speed gas turbine engines (e.g. the T800).

HIGH SPEED ROTOR DEVELOPMENT

The emphasis in today's helicopter rotor development is high speed, with low vibratory loads and low noise. To this end, Boeing Vertol is conducting a multi-disciplinary program to gather the test evidence and develop the methods necessary to design better rotors. The feasibility of improving upon the current generation of advanced rotor systems is considerably enhanced by recent advances in computational methods and testing techniques.

ADVANCED ROTOR DEVELOPMENTS PRIOR TO 1982

As summarized in Reference 1, a family of airfoils optimized for use on high speed rotors was designed and tested in 1978. These airfoils, the VR-12 to VR-15 sections, were defined for high Mach number penetration on the advancing side without compromising the high lift performance necessary to avoid dynamic stall over the retreating side. Wind tunnel tests of rotors employing the new sections started shortly after the 2-D airfoil tests.

An extensive series of advanced rotor wind tunnel tests was carried out in the Boeing Vertol Wind Tunnel (BVWT) between 1978 and 1982. These tests, summarized in Reference 2, demonstrated that conventional helicopter rotors can be flown at speeds beyond 200 knots while still producing useful lift and propulsive force. One configuration was tested up to 231 knots, the speed limit of the wind tunnel. Figure 11 shows one of the model rotors installed in the BVWT. Of all the configurations tested at that time, the one that achieved the best compromise between performance and loads employed the new family of high speed airfoils and a 3:1 chord taper over the 10 percent of span. This rotor was selected for the Model 360 helicopter.

The advanced rotor tests in the BVWT showed the straight, tapered tip configuration to be better than other configurations employing various amounts of tip sweep. That conclusion will be re-evaluated periodically, considering such recent developments as those reported in Reference 3. For the present, the Model 360 rotor system is the best of all those that Boeing Vertol has evaluated in the wind tunnel. It will be flight tested in 1987, and it is the baseline for the investigation of more advanced rotors.

During the advanced rotor wind tunnel test program, flight at very high speeds was achieved at the cost of relatively high vibratory hub loads. High speed was not limited by power, but by safety-of-flight limits on the fatigue loads experienced by the model blades and control system. Close examination of the performance and loads near the rotor limits did not yield any useful clues about the fundamental source of the vibratory loads.

NATURE OF VIBRATORY AIRLOADS

A breakthrough in identifying the causes of the vibration experienced by helicopter rotors in high speed flight came with a re-examination of existing NASA test data for the H-34 rotor. As described in Reference 4, a detailed time history of blade airloads, obtained by integration of

measured surface pressures, can be harmonically analyzed and reconstituted to identify the radial and azimuthal extent of the loads associated with different harmonic components. Figure 12 shows an example of a cartesian, isometric display of the H-34 data as measured in Reference 5. Complete airloads (harmonics 0 to 10) and vibratory airloads only (harmonics 3 to 10) are presented. Clearly, the largest vibratory airloads occur at the tip as the blade travels from the first to the second quadrant. To the extent that they are a forcing function driving the vibratory response of the entire helicopter, any reduction in these airloads should result in a reduction in the overall rotor induced vibration.

Although the design of low-vibration rotors depends on the prediction of vibratory airloads, none of the rotor analysis codes available in 1983 produced satisfactory predictions. This lack of agreement between test and theory is illustrated in Figure 13, from Reference 4.

DEFINITION OF APPROACH

Between 1983 and 1984 systematic attempts were made to quantify the mechanism behind the vibratory airloads observed in the H-34 data. The main cause of the poor predictive capability was finally determined to be the incorrect modeling of the rotor wake over the advancing side of the disc.

As illustrated in Figure 14, the tip of the advancing blade of a rotor in high speed flight experiences negative loading. This negative loading is the source of trailed vorticity of negative sign, but the wake models available at that time did not have provisions for regions of locally reversed vorticity.

The following approach was proposed to understand and reduce the wake effects contributing to vibratory airloads:

a) Gather experimental evidence on the structure of the wake and on the magnitude and phase of the vibratory airloads.

b) Develop more representative wake models and integrate them into rotor analysis codes which properly couple all aerodynamic and dynamic effects.

c) Design and demonstrate by wind tunnel test low-vibration and low-noise rotors.

The low noise goals arise from the fact that the wake not only causes vibratory airloads, but is also a significant contributor to the acoustic signature of a rotor. If the interaction between rotor and wake can be changed to reduce vibration, it should be possible to change it to reduce noise.

FLOW VISUALIZATION

The first experimental objective was to confirm that negative loading on the advancing tip results in a discrete region of "negative" trailed vorticity. A towing tank test carried out at Flow Industries, in Kent, Wash., during the fall of 1984 provided this confirmation.

A typical flow visualization record, along with an interpretation of the flow picture, is shown in Figure 15. Reference 6 reports on the most significant test conditions. This was the first test in water of a helicopter rotor model equipped with cyclic controls. The model was a four-blade, 16 inch diameter, geometrically scaled H-34 rotor. The conditions examined in the towing tank test included some of the advance ratios of the original H-34 test, Reference 5.

Although the towing tank records were informative it would have been more desirable to investigate the rotor wake in air, but flow visualization (and measurement) in air for forward flight conditions at realistic tip speeds has been, so far, disappointing. There is some hope, however, because promising new techniques have been recently perfected which will make it possible to carry out instantaneous rotor wake measurements.

ADVANCED WIND TUNNEL TESTS

Between 1982 and 1985, a rotor set of dynamically scaled and pressure gage instrumented model blades was designed and built at the Boeing Vertol Wind Tunnel. This rotor, a 1/5 scale model of the Model 360 rotor, was tested in February 1985. Only a limited amount of data was acquired because of instrumentation difficulties, but the measured airload distributions were in qualitative agreement with the airloads from the H-34 test. Figure 16 shows two typical airload distributions. More details about this test are presented in Reference 7.

A new set of blades was built between 1985 and 1986. In this blade set, the reliability of the pressure transducer installation was greatly improved. The new blade set, shown in Figure 17, was successfully tested in a joint Army/NASA/Vertol aeroacoustic program at the Duits Nederlandse Windtunnel (DNW), during the summer of 1986. Digitized and finally reduced data will be available by mid-1987.

In the DNW tunnel, testing was carried out up to a speed of 199 knots. From a preliminary review of the data it appears that most of the pressure instrumentation, including the tip pressure gages, operated correctly throughout the test.

ROTOR WAKE MODEL DEVELOPMENT

Key features of the B-65 rotor performance and airloads analysis are shown in Table 1. Until recently, the wake models in B-65 and other Vertol rotor codes were "kinematic", namely their geometry was determined on the basis of blade motions, inflow velocity and averaged induced downwash without any wake distortion, or free-wake, effects.

- Lifting-line model
- Azimuthal resolution options (increments between 5 and 15 degrees)
- Spanwise resolution of up to 39 stations
- Uniform and non-uniform downwash
- Betz rollup approximations
- Kinematic and free (CDI) wake options
- Delayed rollup vortex sheet (trailed and shed)
- Articulated and rigid rotors
- Two-dimensional airfoil data base
- Unsteady aerodynamics/Dynamic stall delay
- Three-dimensional tip relief effects
- Tip sweep model
- Elastic properties by modal representation
- Flapping and flap bending by either time or frequency domain solution
- Upwash/interference effects
- Time-averaged and instantaneous performance and airloads
- Provisions to interface with other codes

Table 1 - Key features of the B-65 forward flight rotor analysis

During 1984, systematic calculations involving the kinematic wake models were carried out to investigate how the wake roll-up assumptions influenced the prediction of vibratory airloads. The conclusion was that no roll-up is better than the wrong roll-up. The use of extended (delayed roll-up) vortex sheets yielded airloads which were low in amplitude but otherwise in excellent agreement with the measured data. This was the evidence necessary to initiate the development of wake models with more representative far-wake vorticity distributions, including the modeling of the wake trailed by negatively loaded blade tips. Two options were available:

(1) To modify the existing kinematic wakes so that multiple (more than two) vortices could be introduced wherever necessary.

(2) To formulate a totally new model, including free-wake effects.

The decision was made to do both. The kinematic wakes were modified in-house, while the development of the free wake was subcontracted to Continuum Dynamics, Inc., (CDI), of Princeton, N. J., and Dr. D. Bliss from Duke University.

Although much effort has been directed to the development of free wakes, free wakes are not always necessary. Kinematic wake models are useful when the wake is not too close to the rotor blades. This is generally the case when the rotor produces a significant propulsive force. It is not true at small tip path plane angles when the propulsive force is small. The changes to the kinematic wake model were conceptually simple: options were introduced for various distributions of rolled up far wake vortices, with a maximum of ten, and a substantial improvement was observed in the agreement with the H-34 data.

When the flow causes the wake to move close to the rotor blades it becomes necessary to account for local wake distortion effects. While past experience with free wakes had been disappointing because of poor convergence and high costs, the CDI model includes new features which considerably improve the efficiency and accuracy of the wake calculations, particularly in addressing vibratory airloads.

Figure 18 illustrates the key characteristics of the CDI wake. The main advantages are:

- The use of curved vortex elements. These allow the modeling of the wake with few vortex segments where a larger number of straight segments would be needed. The use of curved elements also simplifies the calculation of self-induced wake distortion effects.

- The modeling of the wake by a system of lines of constant vorticity, not separating trailed and shed vorticity components. In the presence of large gradients the vortex lines are closely spaced. Widely separated lines indicate regions with low gradients.

One small difficulty is that the wake does not originate at fixed collocation points along the blade and therefore a near wake has to be introduced to provide some transition between the blade and the body of the wake.

Computer assisted graphics have been used to display both the wake geometry and the associated induced velocity field. Figure 19 is an example of the CDI wake geometry as introduced into B-65. A computation grid perpendicular to the disc plane and passing through the blade shows the in-plane components of the velocities induced by the all the vorticity in the rotor flow field for that particular rotor position. Figure 20 shows the instantaneous velocities induced on a rectangular computation grid along the disc plane. These displays were developed to assist in code checkout and test/theory correlation.

TEST/THEORY CORRELATION - H-34 DATA

Because of the new kinematic and free wakes, considerable improvements have been made in the prediction of vibratory airloads. Figure 21 compares the measured and calculated vibratory airloads for the same condition shown earlier in Figure 13. The agreement between test and theory is now good. Although both the CDI and Betz wake models require further improvements to make them more generally useful, it is finally possible to examine by analysis candidate low-vibration rotor configurations.

LIMITS OF THE LIFTING LINE APPROACH - BVI MODELING

Significant efforts are under way to model helicopter blades as three-dimensional lifting surfaces, but, as promising as they are, the new Computational Fluid Dynamics (CFD) codes cannot be used without the wake and inflow information currently provided by lifting line rotor codes. Figure 22 summarizes the blade/vortex proximity effects of concern in determining the range of validity of lifting line rotor analysis methods. The only instance in which lifting line and discrete-vortex wake models are correct without any empirical adjustment is when the separation between wake and blade is at least one chord. At distances of less than one chord the lifting line modeling becomes increasingly questionable. Events leading to an actual encounter between blade and vortex cannot be modeled with any degree of accuracy, although useful trends might be producted by introducing empirical considerations.

Methods modeling the full transonic encounter between a vortex and a two dimensional airfoil have been available for some time, but to define low vibration rotors the more localized blade-vortex interaction (BVI) effects did not need to be modeled as urgently as the overall rotor wake. Of more immediate concern has been an assessment of the limits of validity of the lifting line approach. A two dimensional Joukowsky transformation, described in Reference 8, was used for this purpose. Systematic calculations, as shown in Figure 23, were carried out. As mentioned earlier, a preliminary conclusion was that lifting line methods are valid for blade/vortex separation distances of at least one chord, Figure 24. This also means that a free wake model is an essential prerequisite to the correct formulation of the blade/vortex interaction problem, since the modeling of the details of blade vortex proximity effects is not useful until the position of the wake relative to a blade can be accurately estimated.

COUPLING OF B-65 WITH CFD CODES

The evaluation of the transonic flow field over the tip of rotor blades has been a research objective at NASA and Army Research Centers for years. Boeing Vertol, as the other helicopter manufacturers, has been following with great interest the CFD developments. Early versions of the CFD codes were acquired and tried as soon as they became available. These codes are:

- ROT-22, a NASA/Ames modification of FL022, Reference 9,
- TFAR-1 and TFAR-2, more recently developed at NASA/Ames, References 10 and 11,
- FDR, developed at the Army's Aeroflightdynamics Directorate, Reference 12.

Euler and Navier-Stokes solvers are being currently developed and will become operational over the next few years.

What these codes have in common is that they can evaluate the flow field around a rotor blade, one azimuth position at a time, as long as boundary conditions can be defined from an external source. What these codes cannot do is to:

- Relate the flow field to the forces a rotor has to produce to maintain a given flight condition,
- Couple the airloads with the flapping motions and elastic deflections of the blades,
- Evaluate the rotor wake.

Wake effects, blade motions and deflections, rotor forces and suitable boundary conditions are obtained from lifting-line rotor analysis codes. At Boeing Vertol the information necessary to carry out CFD rotor calculations has been produced by means of the B-65 rotor analysis code. Open-loop coupling only has been attempted so far, with very encouraging results.

Recent calculations carried out by means of the FDR, TFAR-1 and TFAR-2 codes to match test conditions from a pressure instrumented blade test are described in Reference 7. Figure 25 is an example of pressures calculated by means of B-65/TFAR-1 for comparison with test data from the BVWT. Plans are being made to implement soon some form of closed-loop coupling involving B-65, with the CDI free wake, and the CFD rotor codes.

INVESTIGATION OF LOW-VIBRATION ROTOR CONCEPTS

Systematic B-65 calculations have been started to investigate the feasibility of low vibratory airloads rotors. The CFD codes will be used to better understand and model the tip flow environment so that, when possible, more accurate empirical models can be defined and introduced in the lifting line codes.

An example of vibratory airloads trends obtained by means of the B-65 analysis is shown in Figure 26. A parametric study of useful low vibratory airloads trends is the first step in the definition of the next generation of advanced helicopter rotors.

MODEL 360 ADVANCED TECHNOLOGY HELICOPTER

The Boeing Model 360, shown in Figure 27, is unique by virtue of its extensive use of composites. Combinations of glass and graphite are utilized in the blades, hubs, controls, rotor shafts, airframe, and landing gear components. The application of advanced materials is coupled with a high-performance rotor and modularized assembly techniques to provide a focal point for technology development at Boeing Vertol. This section of the paper reviews components developed as part of the Model 360 Advanced Technology Helicopter Program.

ADVANCED HIGH SPEED ROTOR

The construction of the Model 360 rotor blade, shown in Figure 28, is similar to that of the CH-47 and CH-46 currently in fleet use. The basic structural element is the spar, which is composed of unidirectional fiberglass for axial stiffness and strength. To provide the torsional stiffness required for flight at high speed the blade is covered with bias-plies of fiberglass/graphite.

Developed with the support of 4,720 hours of wind tunnel testing, the blade incorporates the VR12/VR15 airfoils, the latest step in transonic airfoils, together with a tapered tip planform. Model rotor tests substantiated the significant performance improvement, shown in Figure 29, available from from the rotor. As shown, the hover efficiency is improved by 6 percent and the cruise efficiency by 23 percent relative to current rotor systems. This rotor, in combination with the low drag Model 360 fuselage, will provide a cruise speed capability of 200 knots.

COMPOSITE DRY ROTOR HUB

The Model 360 hub, shown in Figure 30, has evolved from all glass to mixed modulus construction. A combination of glass and graphite was chosen to meet stiffness and fail-safety requirements.

Primary load paths are through composite structures and elastomeric bearings. Continuous wound hybrid tension loops support the elastomeric flap and lag bearings. These non-viscous bearings do not require lubrication and are expected to provide a significant reduction in mean time to removal relative to rolling element bearings.

Unique to the composite hub is the use of a single hinge for both lag motion and blade folding. This feature provides a significant parts count reduction compared to a three-bladed conventional folding hub. The CH-46 hub and fold mechanism have 1,799 parts; the new four-bladed rotor has approximately 60 percent fewer parts. Due to the reduced parts count and the

use of elastomeric bearings and corrosion-resistant composite material, a 60 percent reduction in maintenance manhours is predicted.

COMPOSITE UPPER CONTROLS

The use of composites has been extended to the upper control system. Benefits of the composites include weight savings, improved fail-safety characteristics, and a corrosion-free assembly. As shown in Figure 31, components such as the swashplate, slider/slider guide, and gimbal ring utilize composite material in their construction. The design is of mixed graphite and fiberglass to achieve approximately a two-fold stiffness increase, compared to metal controls without a weight penalty. Composite construction is coupled with the use of elastomeric rod ends and bearings to avoid spurious vibratory control inputs resulting from deflections.

Graphite content is limited in the control elements and all other mixed-modulus fatigue-critical parts to maintain the soft, safe failure modes and excellent ballistic tolerance of fiberglass construction.

DRIVE SYSTEM

The Model 360 drive system utilizes CH-47 components. Unique to the system, however, are composite forward and aft rotor shafts which are shown in Figure 32. These rotor shafts were chiefly designed to meet stiffness requirements and therefore contain a large fraction of graphite laid at an angle which is effective for both longitudinal stiffness and torsional strength. In addition, circumferential wraps increase bearing allowables at the upper and lower ends. At the upper end, the composite rotor hub is attached by longitudinal bolts connecting to barrel nuts in the wall of the shaft tube. At the lower end, a steel planet carrier is attached to the shaft tube by radial pins.

During static and fatigue tests of the aft rotor shaft, that portion of the shaft which is normally encapsulated in the transmission was heated to 215°F to properly simulate the operating environment.

As a portion of the Model 360 program, composite forward and aft structural transmission covers and sync shafts, shown in Figure 33, were fabricated and tested.

COMPOSITE AIRFRAME

The Model 360 composite airframe, shown in Figure 34, has as its target a 25% reduction in weight, an 86% reduction in parts, and a 93% reduction in fasteners compared to a conventional metal fuselage. Skin panels are composed of KEVLAR skins over a NOMEX core, while the frame and longeron sections are composed of unidirectional graphite caps, NOMEX core, and KEVLAR face sheets. Composites are utilized not only in the skins and frames but in the major support fittings such as the main and nose gear backup structure shown in Figure 35.

The all-composite fuselage was fabricated with a minimum of tools. Skin panels were fabricated in a single cure operation in low cost tools. A single assembly fixture was used to position the ring frames and the longerons. Skin panels were placed in position from the outside. This manufacturing sequence is illustrated in Figure 36.

Cost savings obtained from the use of the Model 360-type tooling/fabrication methods are contained in Figure 37. Model 360 figures are based on results achieved by Boeing during assembly of the primary structure. As compared to conventional metal structure, tooling costs were reduced by 90% and non-recurring costs by 45%.

A shake test of the primary structure including the engines, forward and aft transmission assemblies, and cabin and cockpit floor modules was conducted as part of the Composite Airframe development program. The test showed that the airframe structure meets desired stiffness requirements.

A static proof load test of the primary airframe structure substantiated the ability to meet the planned flight test envelope which includes speeds to 200 knots and maneuvers of 3g's. The composite airframe is shown suspended in the shake and static test fixtures in Figure 38.

MODULARIZED ASSEMBLY

The composite airframe consists of five major subsystem modules, as shown in Figure 39. These subsystems include the tunnel, cockpit, fuselage, nose enclosure, and cabin floor/fuel assembly. The modularization concept greatly reduces manufacturing time and expense.

A unique palletized concept is employed in the Model 360 for mounting the avionics and lower controls. The cockpit pallet, shown in Figure 40, contains avionics and electrical racks, pilots' seats, composite instrument panel, and controls. The pallet, including all the on-pallet wiring, is assembled as a unit outside the airframe.

The cabin floor/fuel system module is of composite sandwich construction using unidirectional fiberglass/epoxy faces for durability and damage resistance. The integral underfloor fuel tanks contain crashworthy fuel cells. The one-piece floor/fuel unit shown in Figure 41 is assembled outside the airframe and the fuel system is pressure checked prior to installation.

Both the cockpit and cabin module are mounted on vibration isolators as illustrated in Figure 42. The entire cockpit module is mounted on four vertical, two longitudinal, and one lateral Improved Floor Isolation System (IFIS) units. These units isolate the cockpit floor from the airframe in the six axes - lateral, vertical, longitudinal, pitch, roll, and yaw. All units are designed for dual frequency operation (isolation at both 4/rev and 8/rev).

Vibration isolation of cargo and fuel is used to prevent fuselage frequencies from passing through resonances at rotor frequencies when large variations in cargo and fuel weight occur. The system is similar to that on the commercial Chinook. It maintains a nearly constant, nonresonant fuselage natural frequency for all fuel and cargo loads while minimizing cabin vibration at the same time.

SUBSYSTEMS

To reduce program costs, proven subsystem components from the Model 234, CH-47D, and CH-46, have been used throughout the Model 360 where feasible.

Subsystems developed for the Model 360 include composite landing gear components, a digital automatic flight control system, a modularized hydraulic system, and an advanced, multiplexed avionics system (see Figure 43).

A fully retractable tricycle gear arrangement was developed as part of the Model 360 program. A unique aspect of the main gear is the use of composites in the construction of the main beams and retraction bellcranks. Constructed of graphite, the beams represent a weight saving of 88 lb compared to steel beams.

The Model 360 cockpit includes an advanced electronic installation developed by the Allied Bendix Aerospace Corporation. Interface with the aircraft and its subsystems is by way of keyboards and electronically generated multifunction displays. The many customary round dial instruments and the warning and caution panels are replaced with multifunction cathode ray tube displays.

Large Scale Integrated electronics and higher order language are used in the Honeywell all-digital automatic flight control system. The system provides tailored command responses and stability as a function of flight condition.

APPLICATION OF MODEL 360 TECHNOLOGY

The technology developed as part of the Model 360 program will result in improvements in performance, maintenance, reliability, availability, and cost. As noted in Figure 44, this technology is providing support to other major Boeing Vertol programs such as the V-22, LHX, and Growth CH-47 in terms of composite manufacturing and assembly techniques and high speed rotor development.

REFERENCES

(1) Dadone, L.; "Rotor Airfoil Optimization: An Understanding of the Physical Limits". Presented at the 34th Annual AHS Forum, Washington, D. C., May 1978. Preprint No. 78-4.

(2) McVeigh, M. A. and McHugh, F. J.; "Recent Advances in Rotor Technology at Boeing Vertol". Presented at the 38th Annual AHS National Forum, Anaheim, Ca., May 1982.

(3) Hopkins, H.; "Fastest Blades in the World". Flight International, 27 December 1986, pp 24-27.

(4) Hooper, W. E.; "The Vibratory Airloading of Helicopter Rotors". Presented at the Ninth European Rotorcraft Forum, September 13-15, 1983, Stresa, Italy. Paper No. 46.

(5) Rabbott, J. P, Lizak, A. A. and Paglino, V. M.; "A Presentation of Measured and Calculated Full Scale Rotor Blade Aerodynamic and Structural Loads". USAAVLABS, TR 66-31, July 1966.

(6) Jenks, M. and Bartie, K.; "Towing Tank Test of a Scale Model H-34 Rotor at Flow Industries, December 1984". Boeing Document No. D210-12356-1, October 29, 1985.

(7) Cowan, J., Dadone, L. and Gangwani, S.; "Wind Tunnel Test of a Pressure Instrumented Model Scale Advanced Rotor". Presented at the 42nd Annual Forum and Display of the American Helicopter Society, Washington, D. C., June 1986.

(8) Poling, D. R., Dadone, L. and Telionis, D. P.; "Blade-Vortex Interaction". Presented at the AIAA 25th Aerospace Sciences Meeting, January 12-15, 1987, Reno, Nevada. Paper No. AIAA-87-0497.

(9) Arieli, R. and Tauber, M. E.; "Analysis of the Quasi-Steady Flow About an Isolated Lifting Helicopter Rotor Blade". Joint Institute for Aeronautics and Acoustics, JIAATR-24, August 1979.

(10) Chang, I-Chung; "Transonic FLow Analysis for Rotors, Part I - Three Dimensional, Quasi-Steady, Full-Potential Calculation," NASA TP 2375, 1985.

(11) Chang, I-Chung; "Transonic FLow Analysis for Rotors, Part II - Three Dimensional, Unsteady, Full Potential Calculation," NASA TP 2375, 1985.

(12) Caradonna, F. X., Tung, C., and Desopper, A.; "Finite Difference Modeling of Rotor Flows Including Wake Effects," Journal of AHS, Volume 29, No. 2, page 26, April 1984.

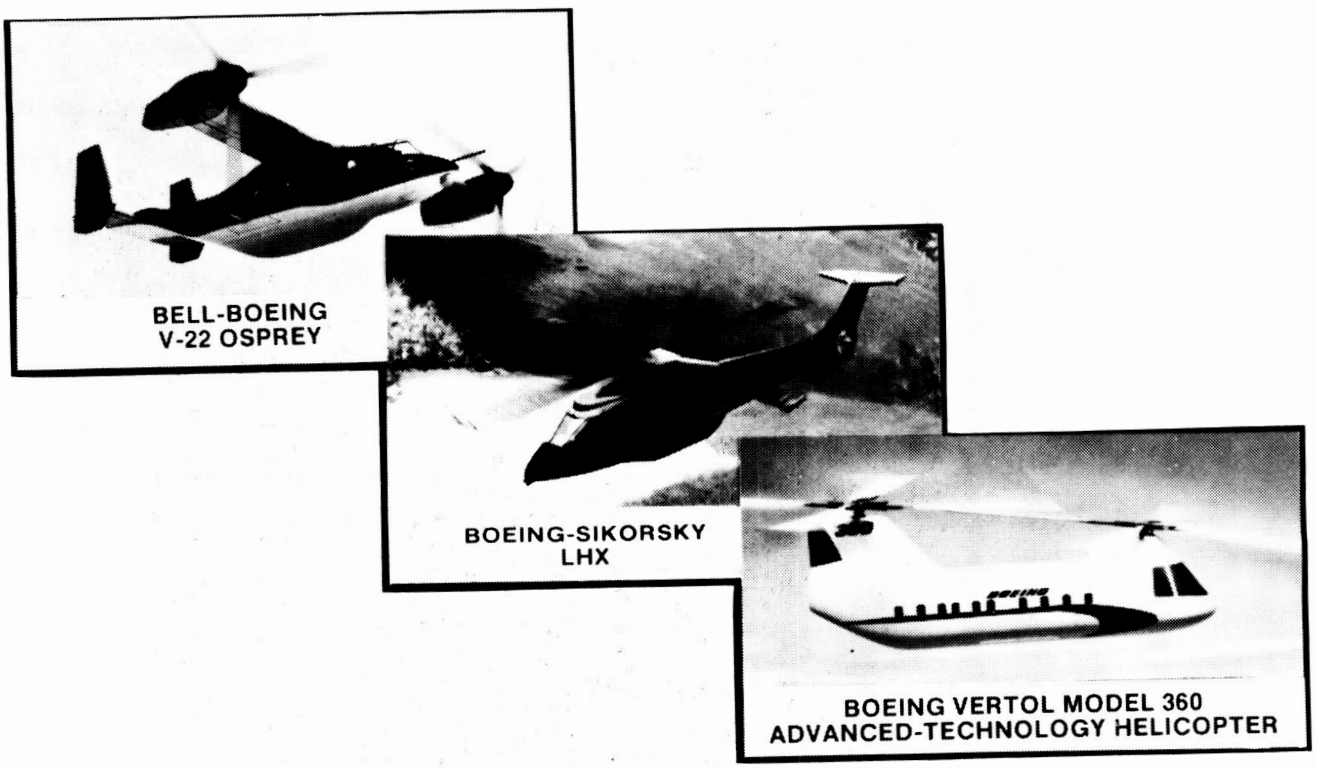

Figure 1. Current Major Programs at Boeing Vertol

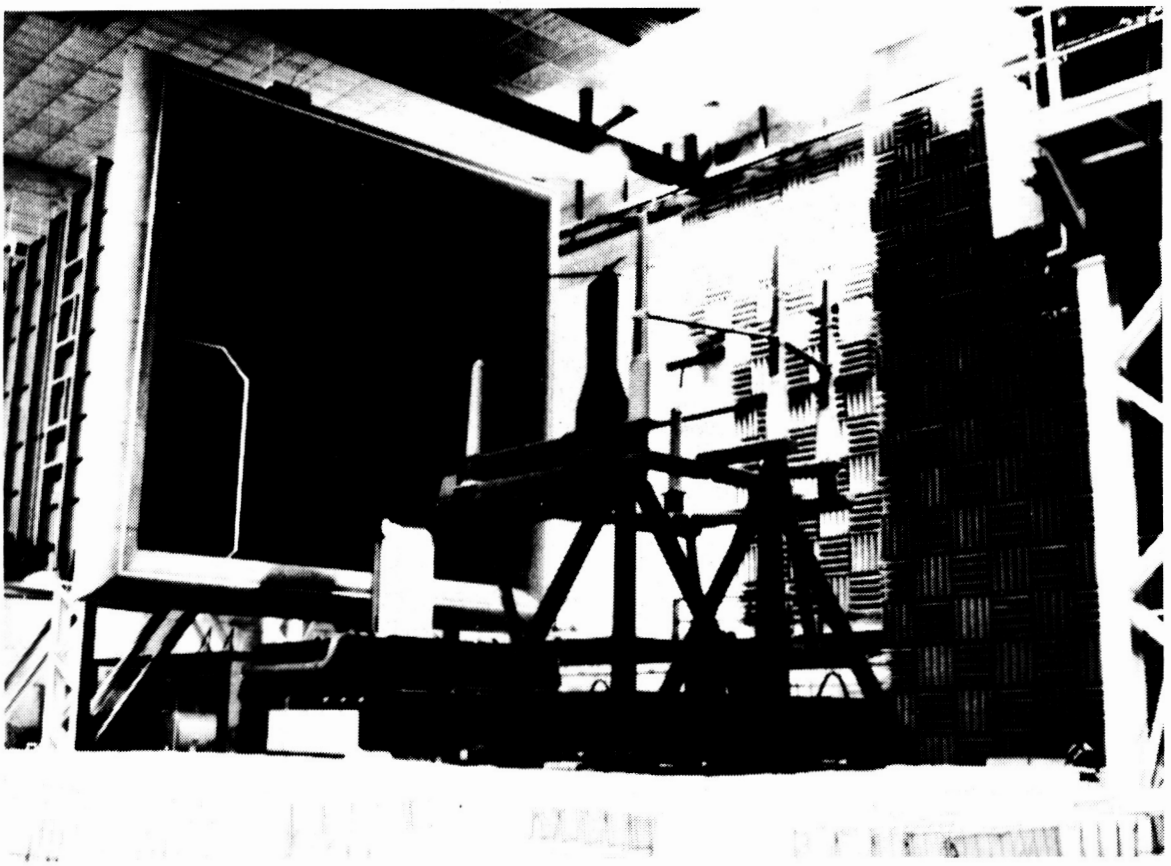

Figure 2. Dynamically Scaled, Pressure-Instrumented Model 360 Rotor Installed in the DNW Acoustic Wind Tunnel

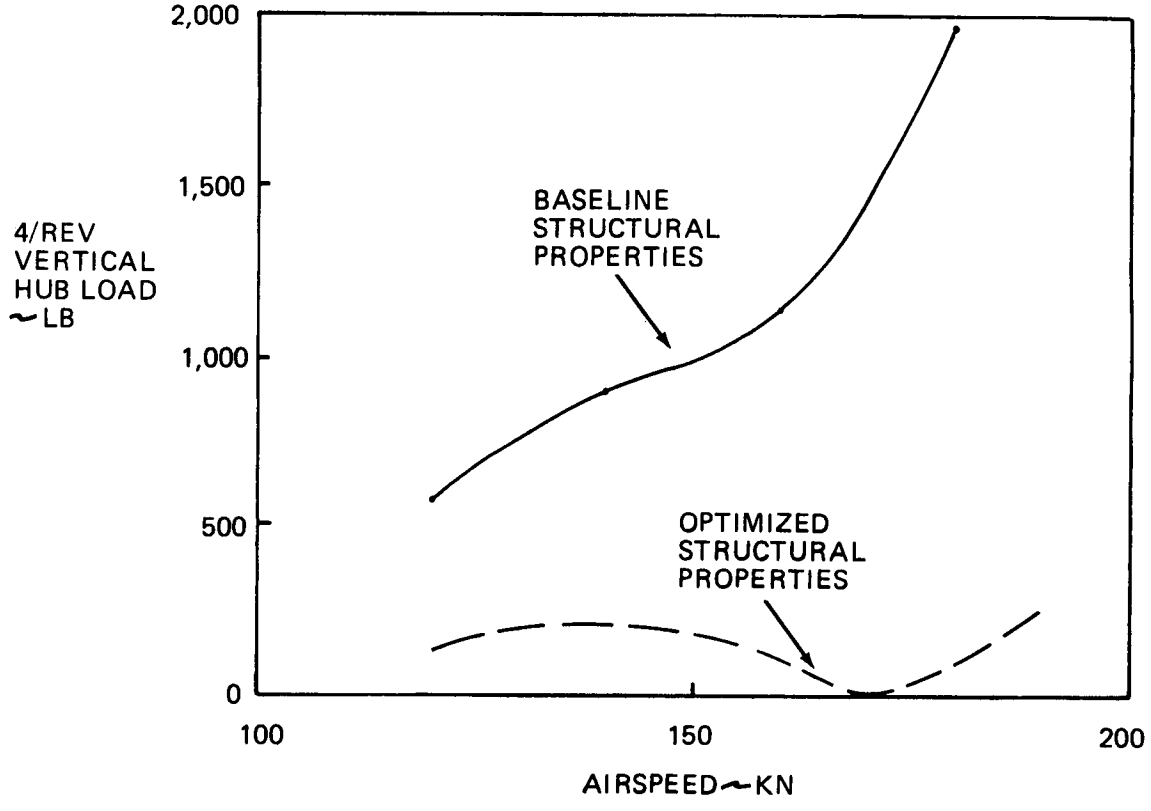

Figure 3. Predicted Vibration-Reduction Benefits of Rotor Blade Structural Optimization

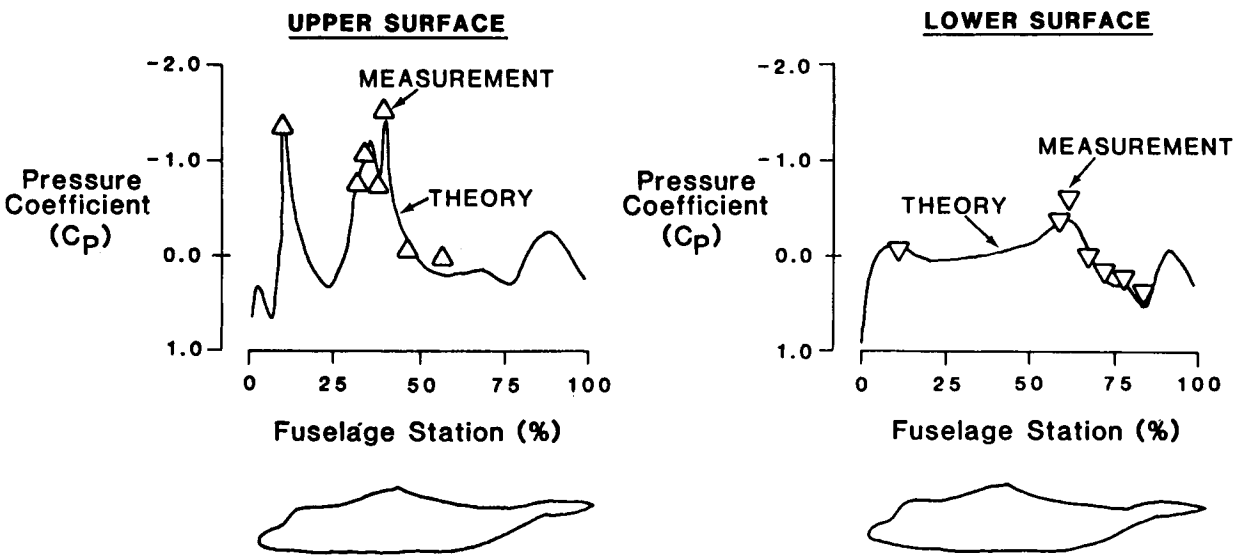

Figure 4. Correlation of Fuselage Pressure Distributions Predicted by 3-D Panel Code and Measured on Wind Tunnel Model ($\alpha = 5^{O}$, M = 0.2, Centerline Pressures)

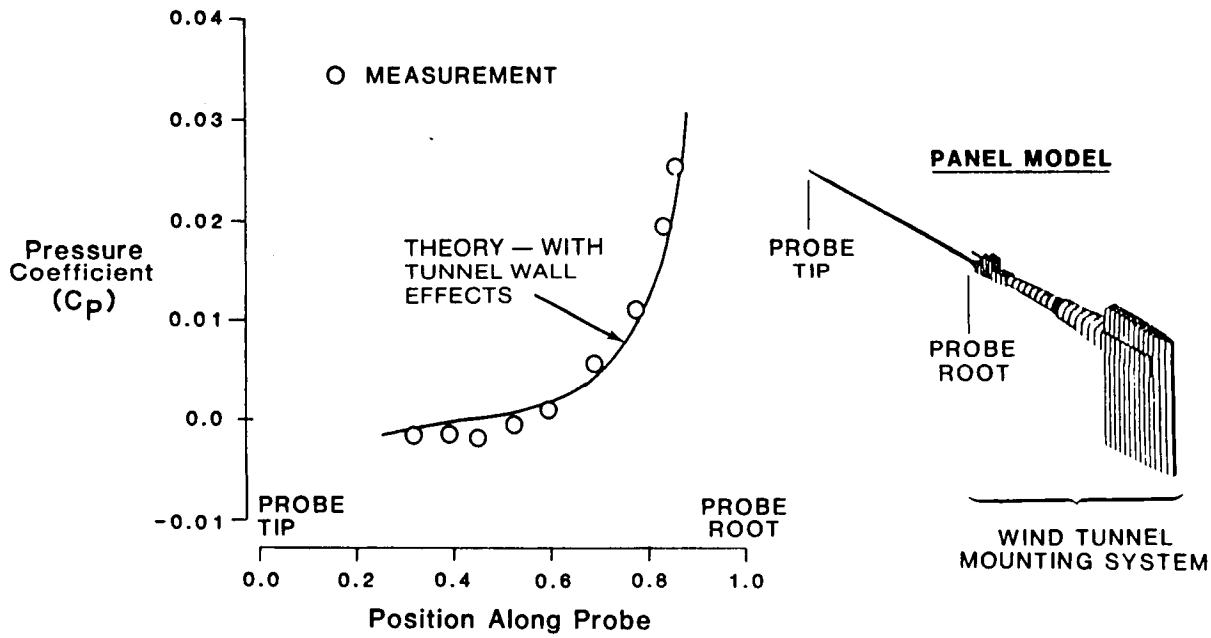

Figure 5. Wind Tunnel Pressure Distribution Caused by Mounting System: 3D Panel Code Prediction vs Measurement

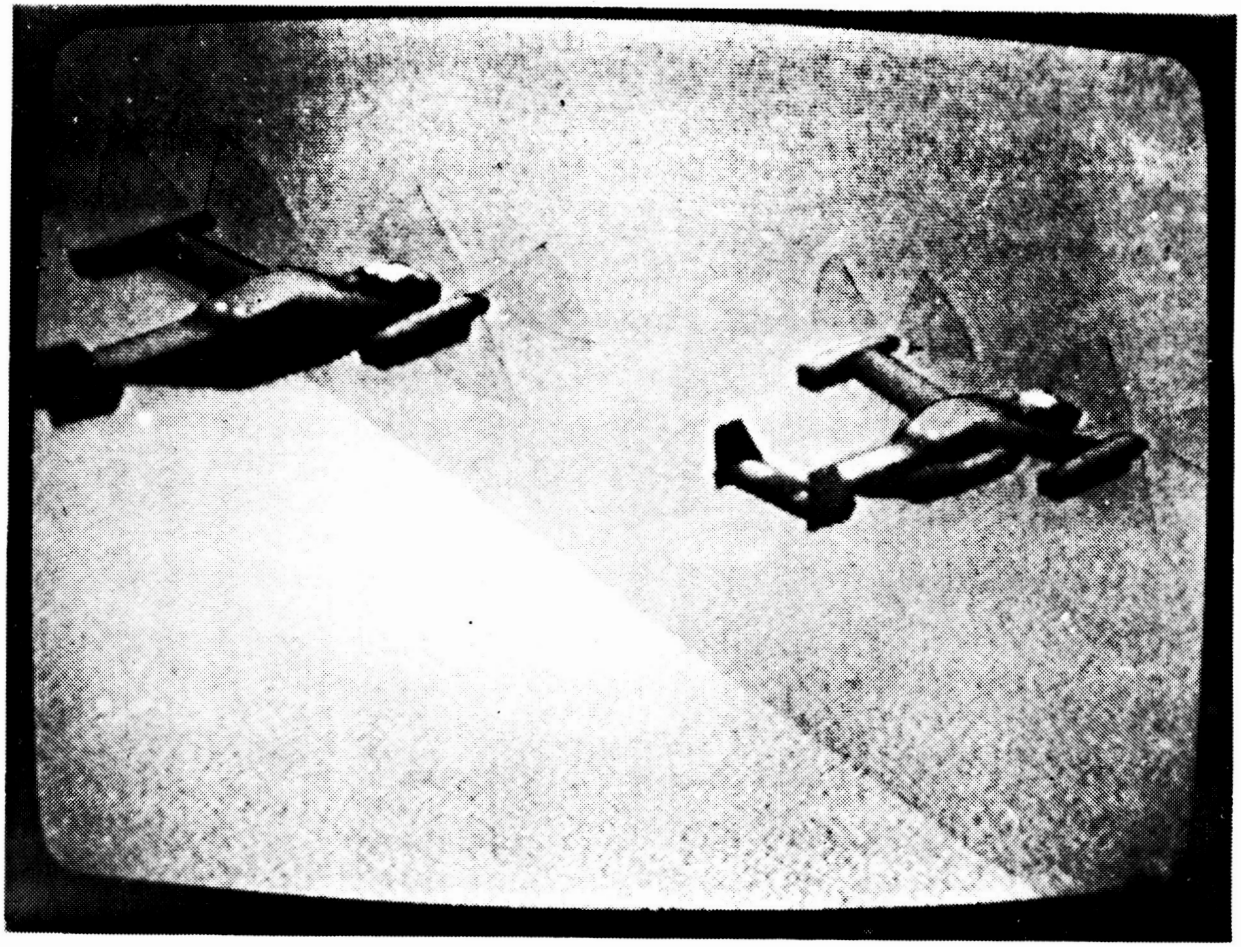

Figure 6. Computer Generated Image from Evans and Sutherland CT6 System Recently Installed in the Boeing Vertol Flight Simulation Laboratory

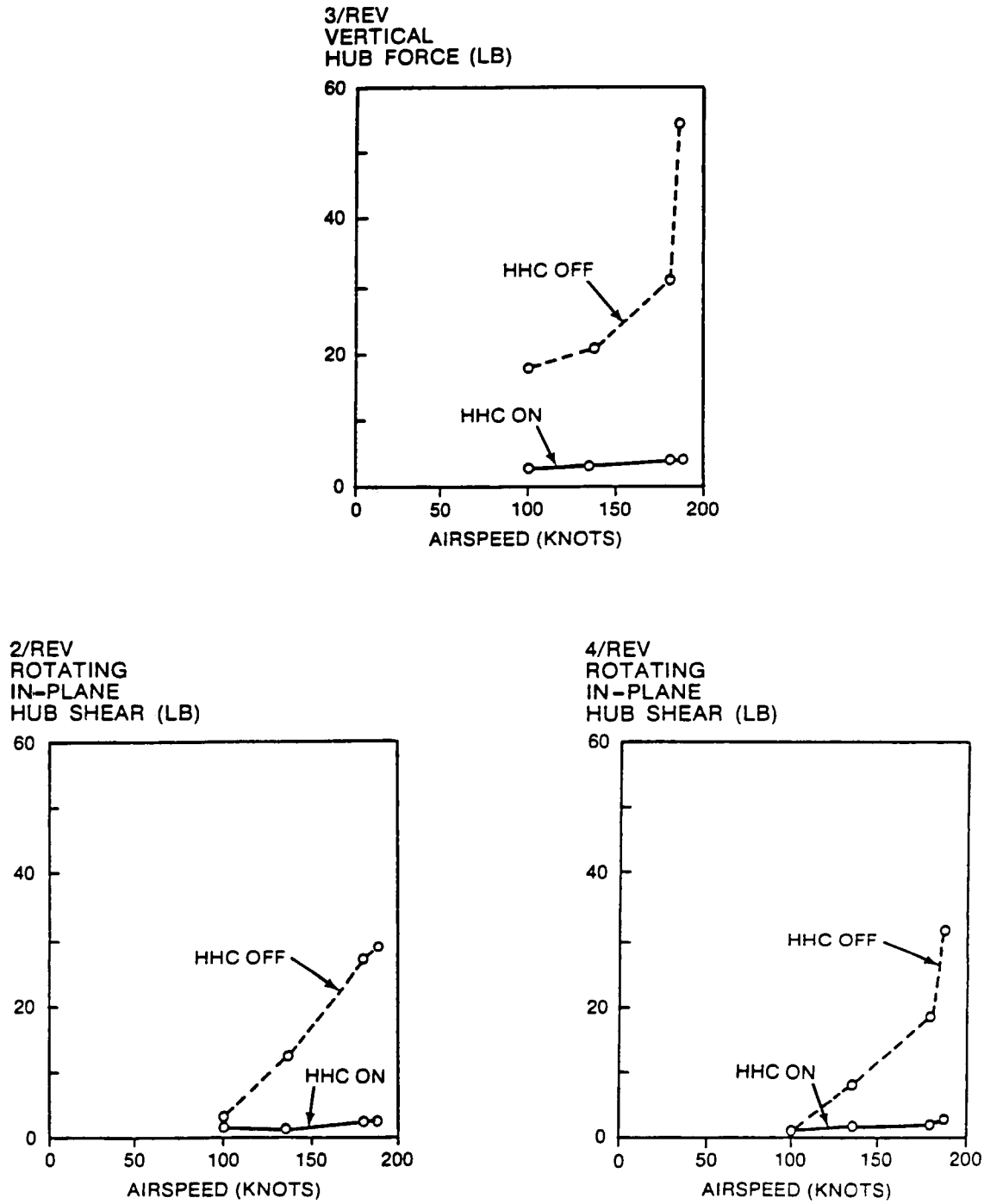

Figure 7. Major Vibratory Load Reduction Demonstrated in the Boeing Vertol Wind Tunnel Using Higher Harmonic Control

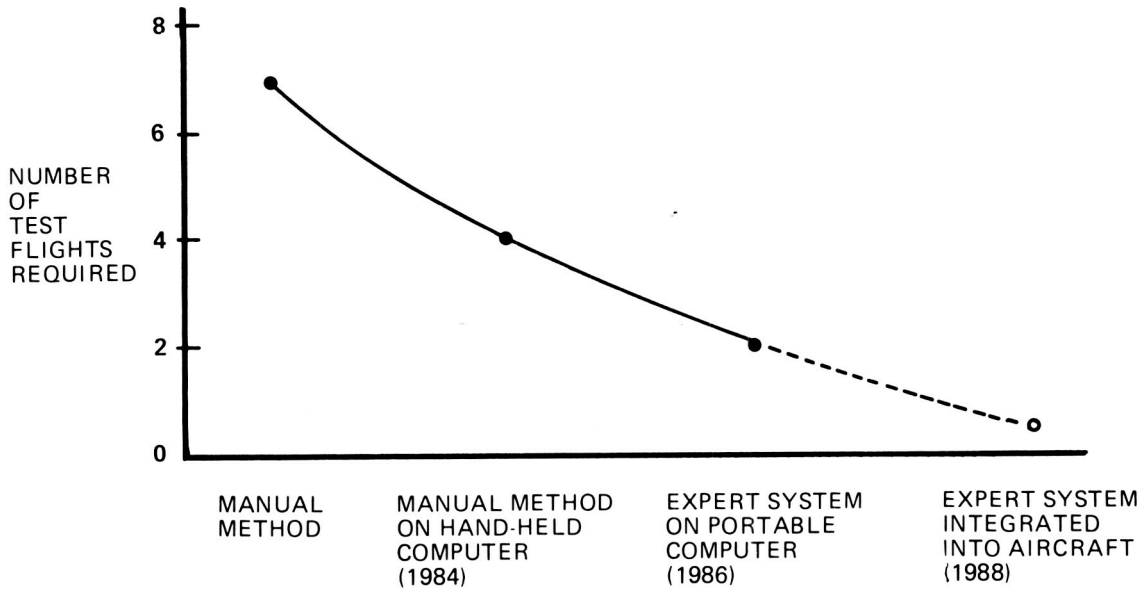

Figure 8. Reduction of Test Flights Required for CH-47D Rotor Track and Balance by Using Expert Systems

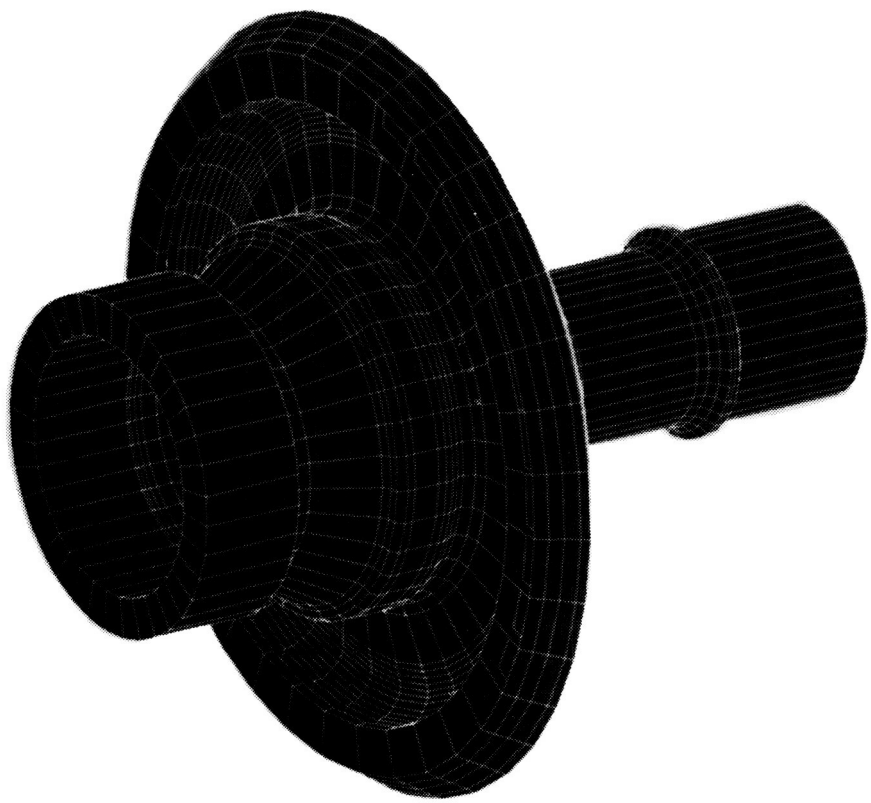

Figure 9. Three-Dimensional Finite-Element Model Used for Design of a Lightweight, Fully Integrated Shaft/Bearing Race/Spur/Spiral Bevel Gear System

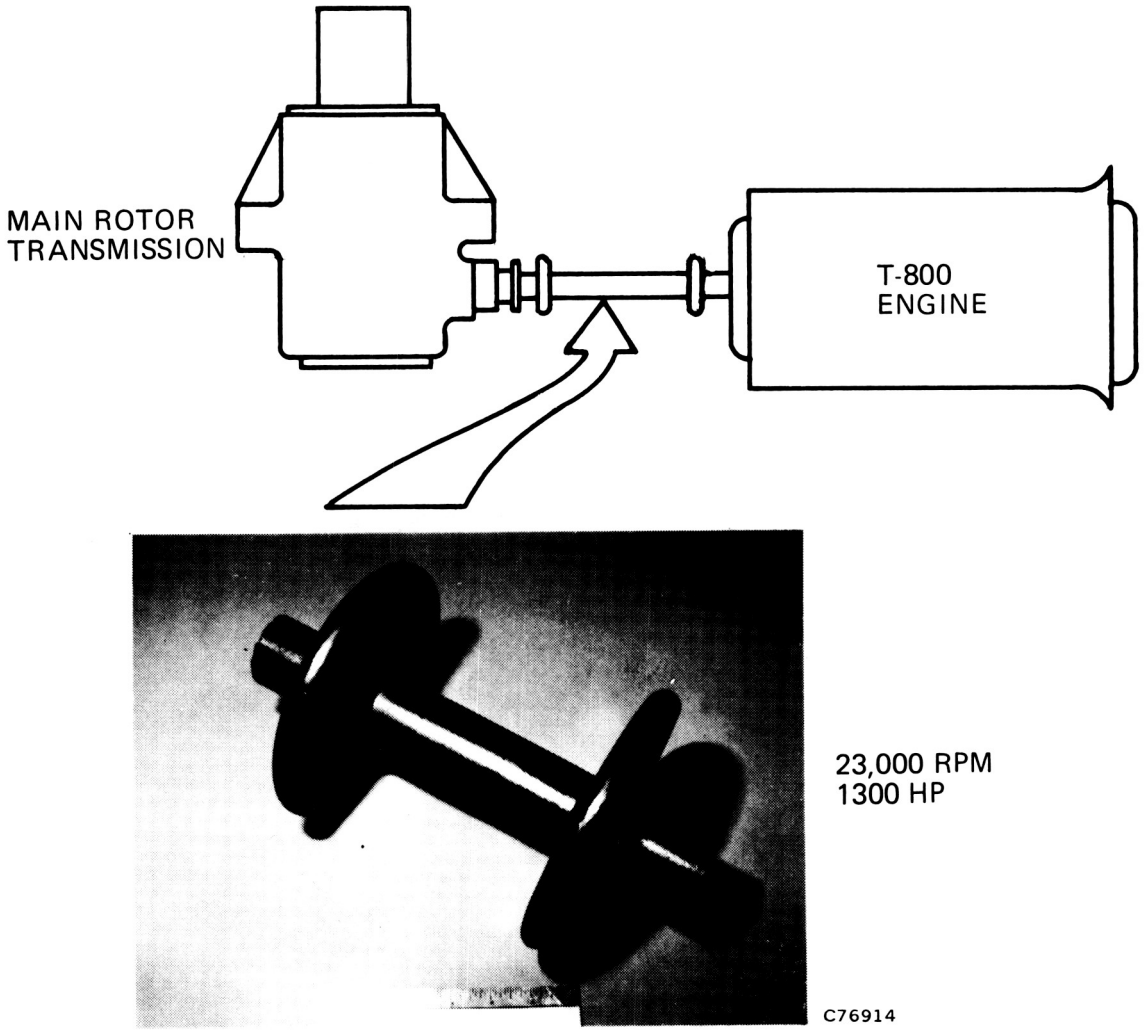

Figure 10. Integrated All-Composite Shaft and Coupling Designed for Large Misalignment Angles

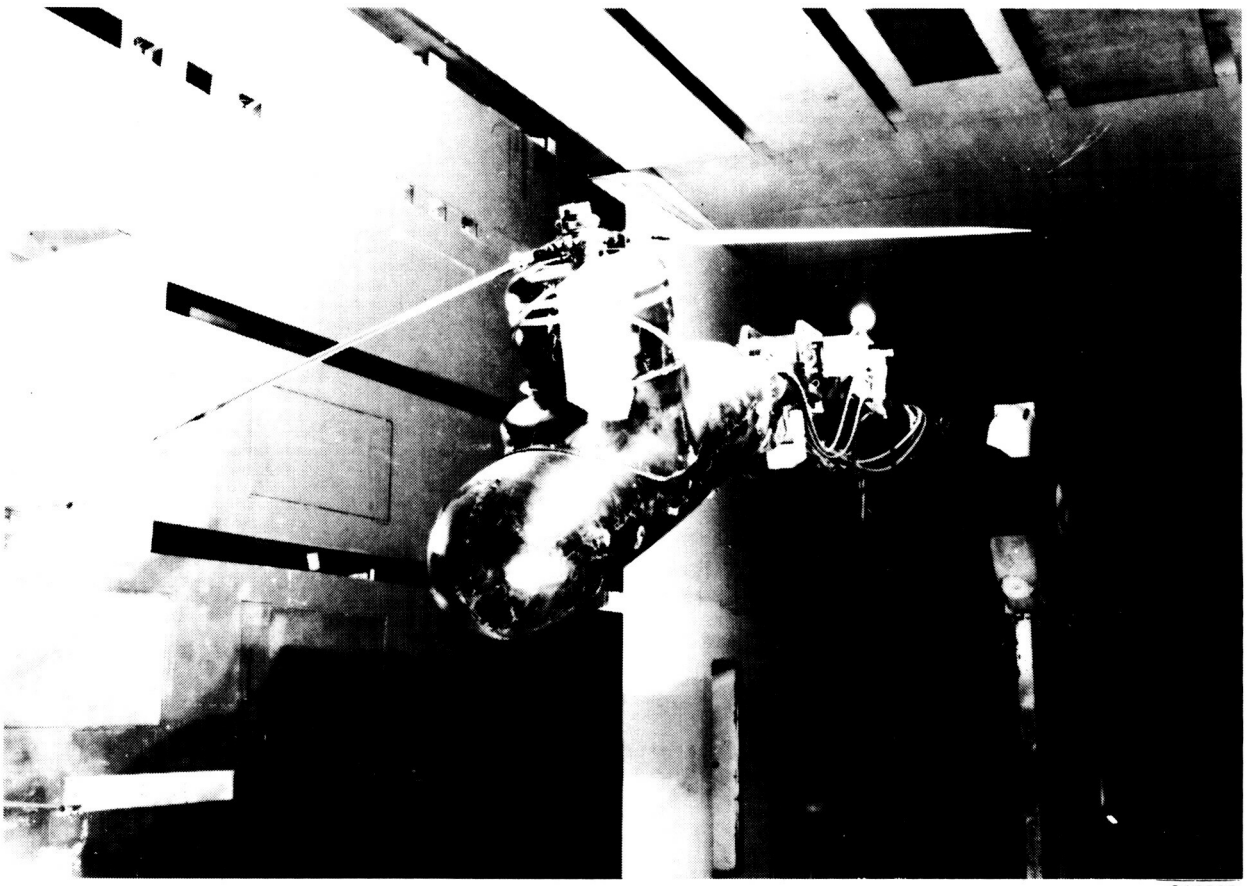

C42537

Figure 11. Single-Rotor Helicopter Model Test Stand

V = 150 KN $\alpha_s = -5^o$ $\mu' = 0.39$

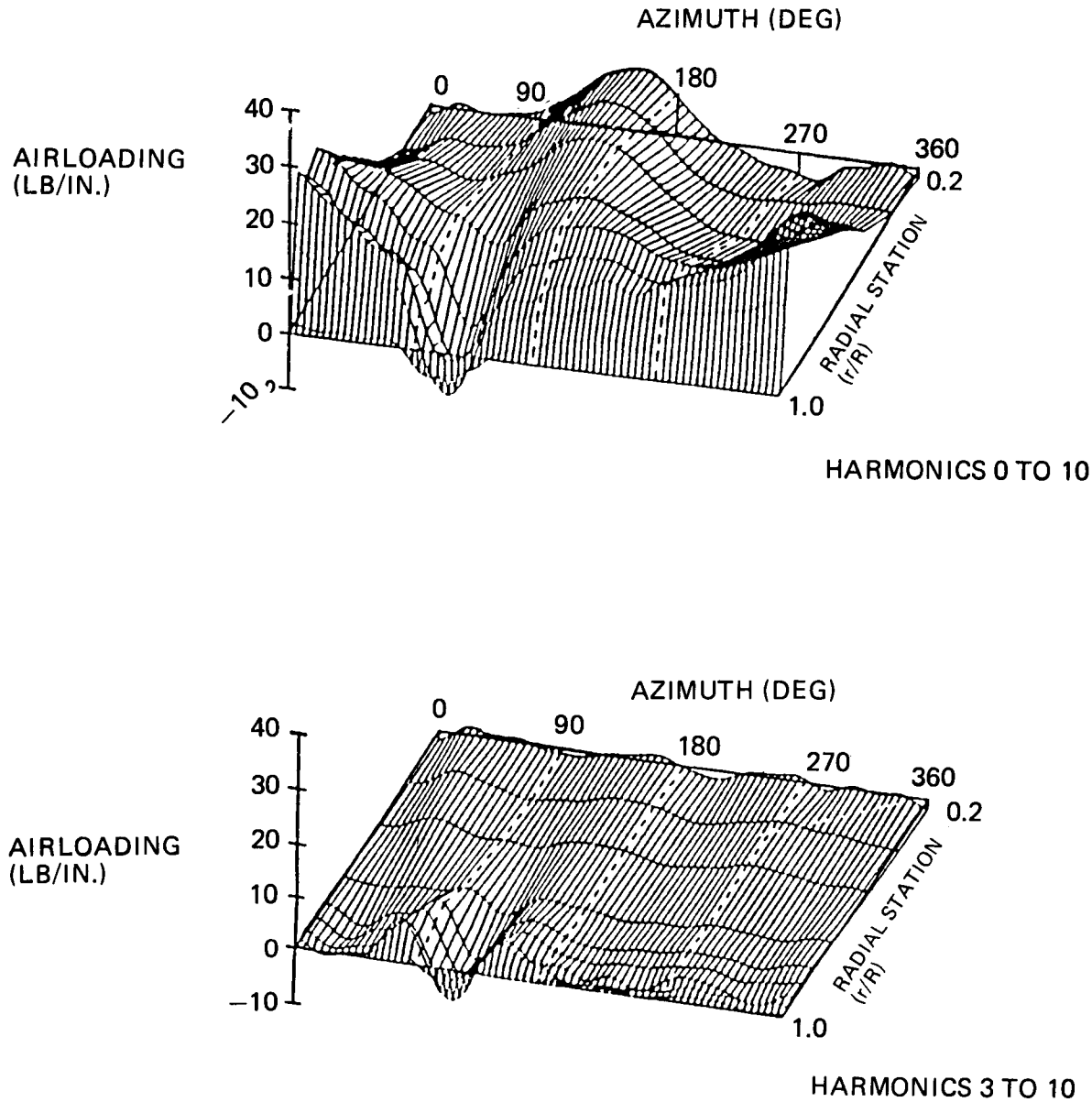

Figure 12. H-34 Data – 150 Knot Case

V = 150 KN
α_s = -5^o
HARMONICS 3 TO 10

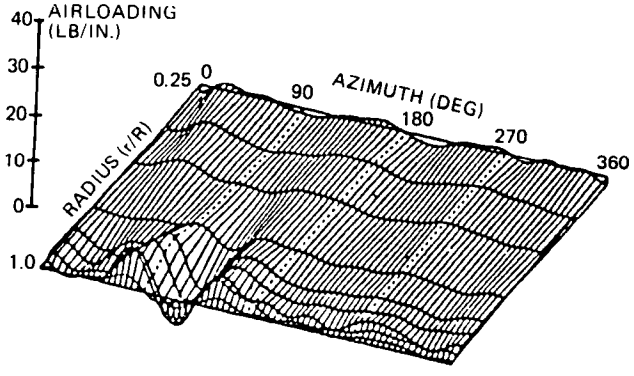

MEASURED AIRLOADING
ON H-34 BLADES

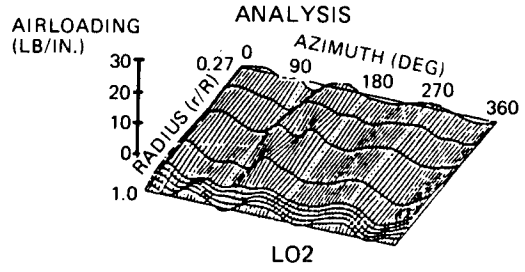

LO2

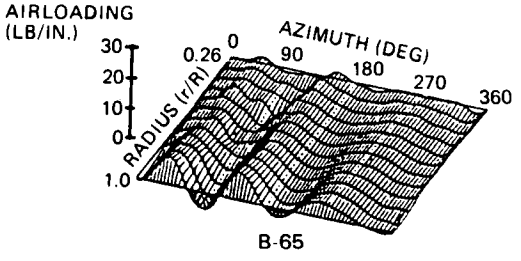

B-65

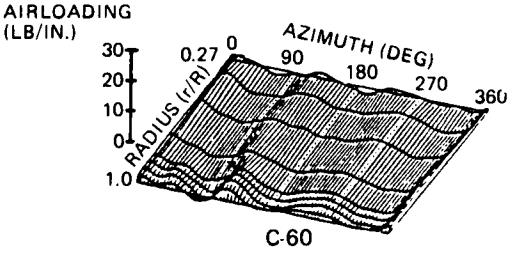

C-60

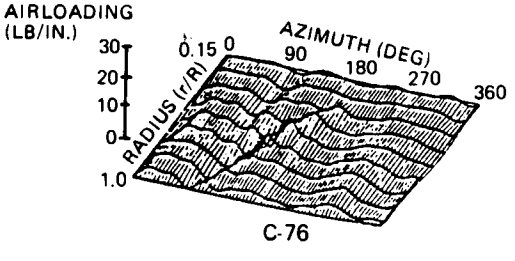

C-76

Figure 13. 1983 Test/Theory Correlation

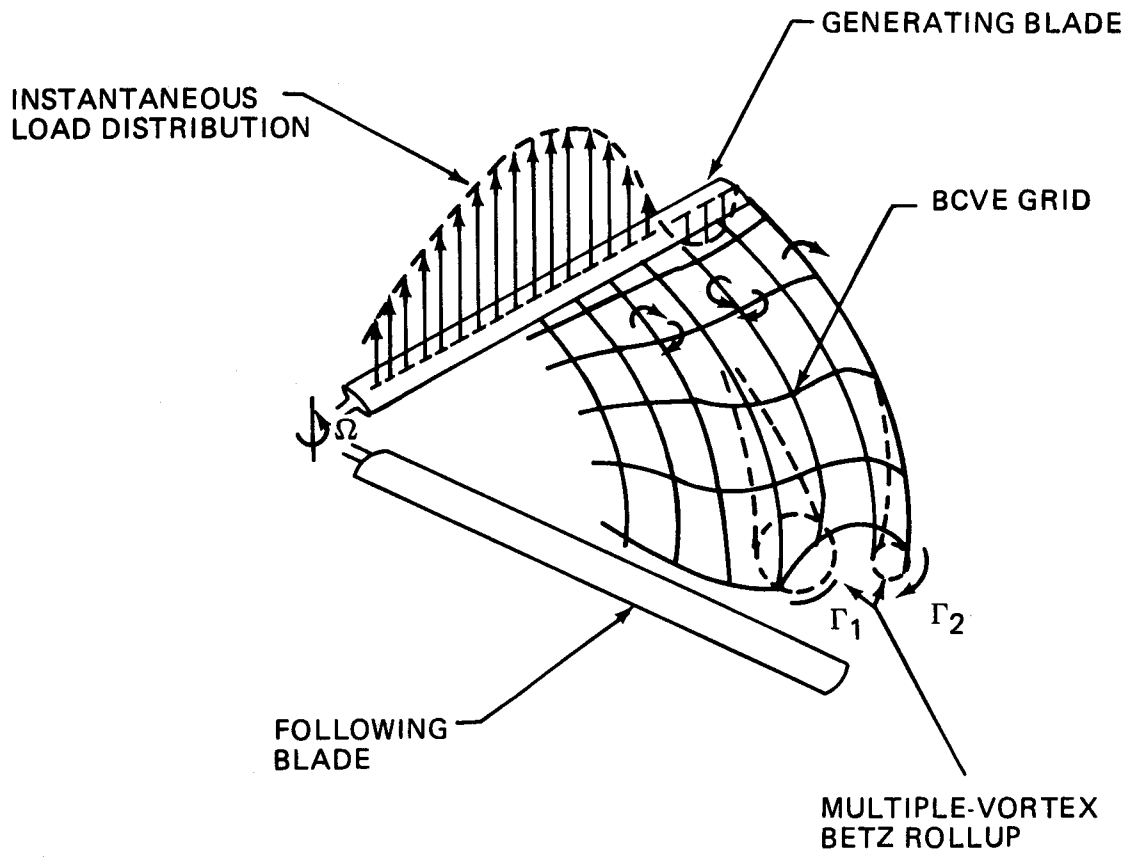

Figure 14. Illustration of Multiple Wake Rollup

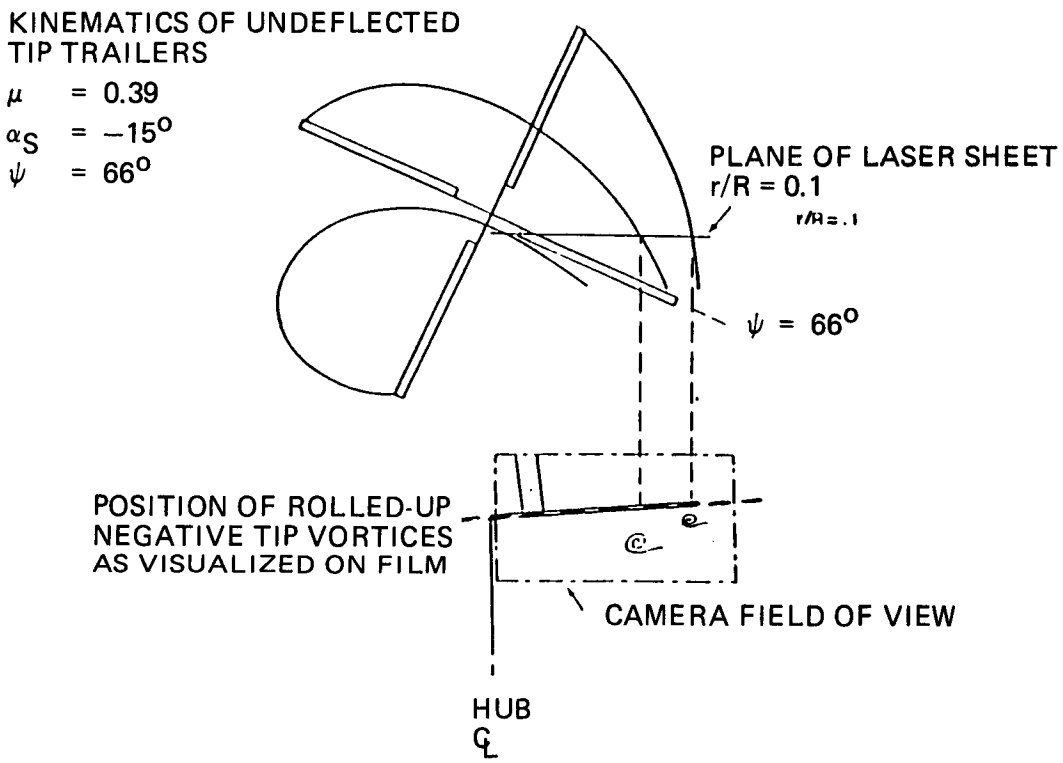

Figure 15. Towing Tank Test Results for H-34 Model Rotor. Example of Wake Kinematics

$C'_T/\sigma_T = 0.07, \bar{X} = 0.05$

BVWT 313 RUN 128 TP 8 $\mu' = 0.35$ V = 146 KN

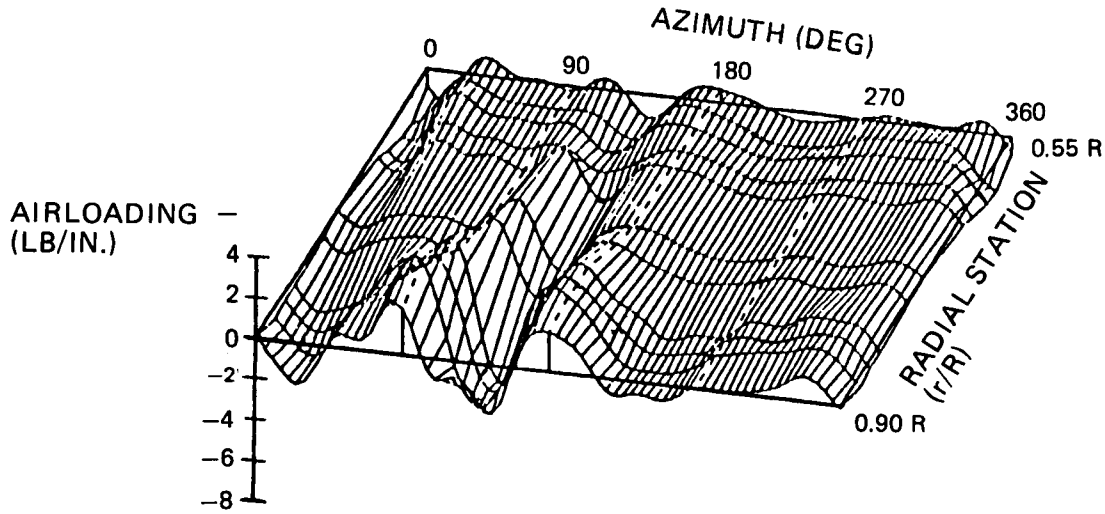

HARMONICS 3 TO 10

BVWT 313 RUN 128 TP 6 $\mu' = 0.25$ V = 104 KN

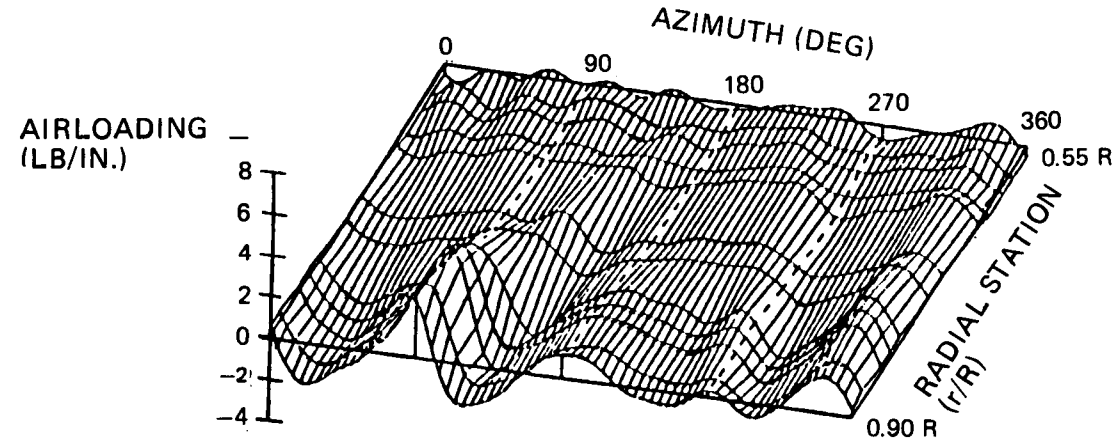

HARMONICS 3 TO 10

Figure 16. Effect of Speed on LE Deduced Blade Airload Distributions

NO. OF ABSOLUTE	NO. OF DIFFERENTIAL	NO. OF WIRES
30	1	78
26	2	72
23	3	72
26	2	72
23	2	72
30	1	78
0	0	0
158	11	(169 TRANSDUCERS TOTAL)

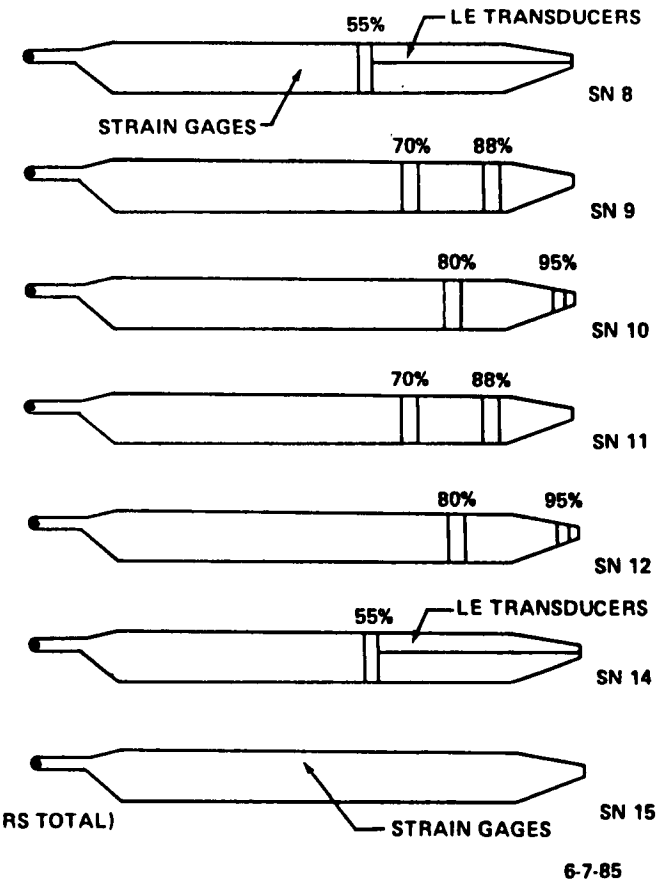

Figure 17. Pressure Blades for BVWT and DNW Tests

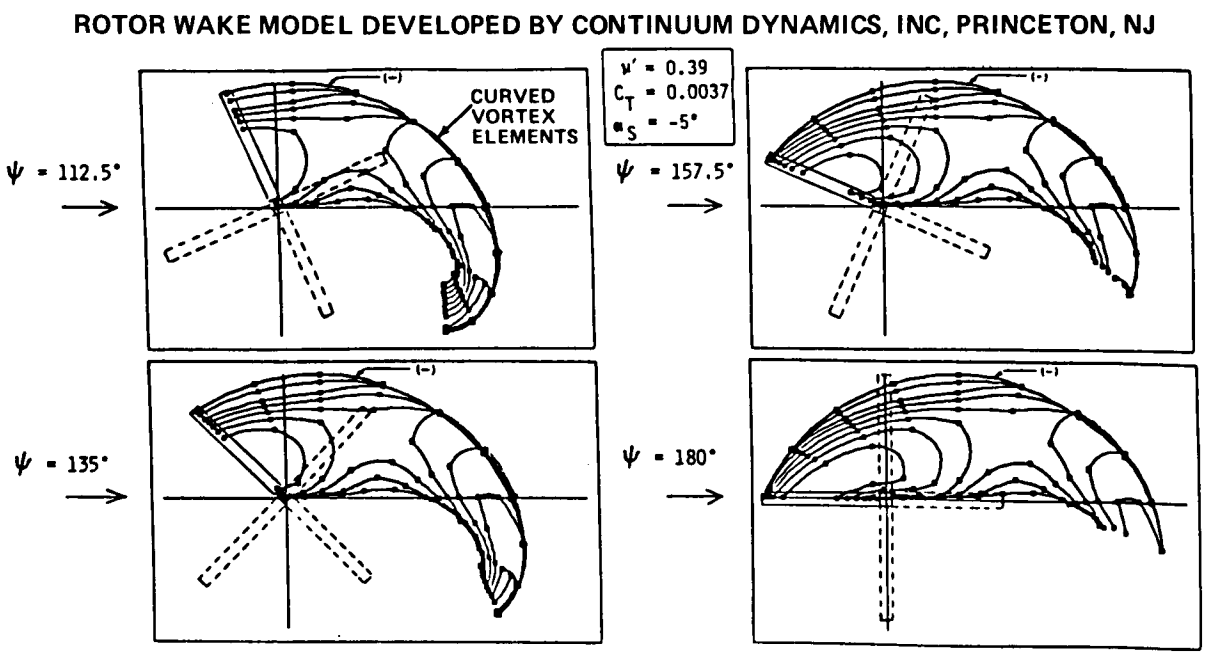

Figure 18. Top Views of Calculated Free-Wake Solutions for the H-34 Rotor (CDI)

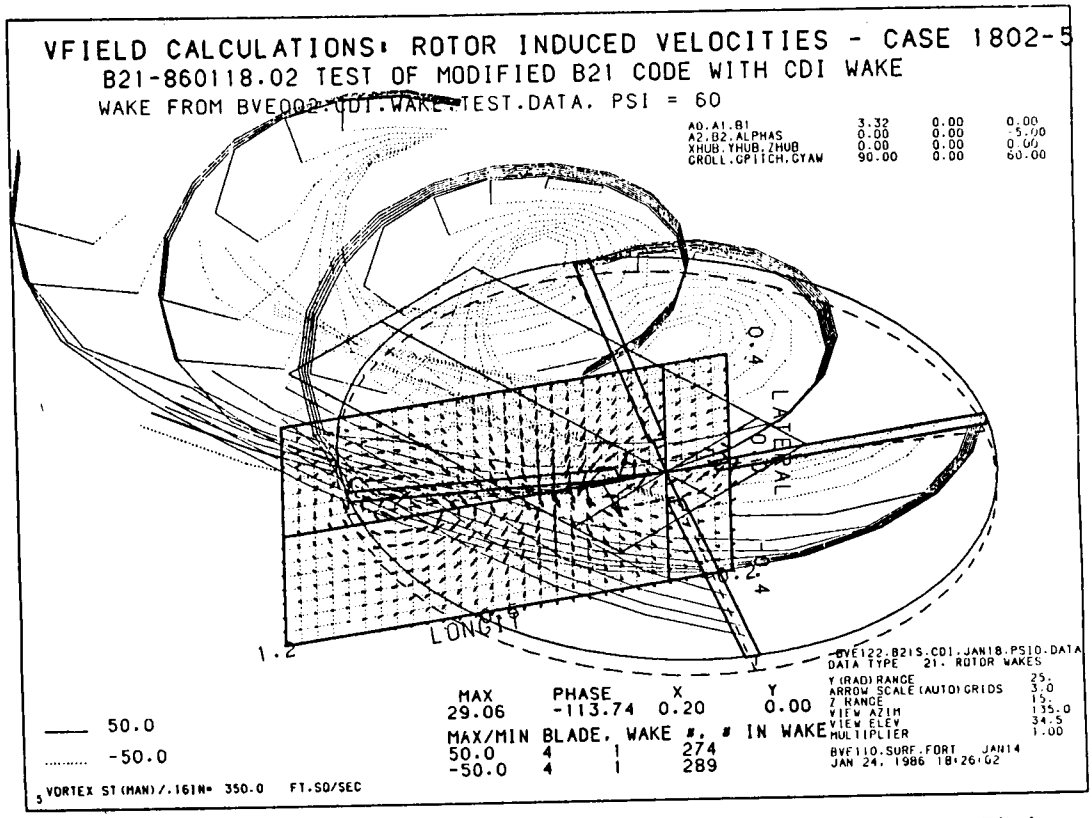

Figure 19. CDI Wake Effect on a Computation Plane Perpendicular to a Blade

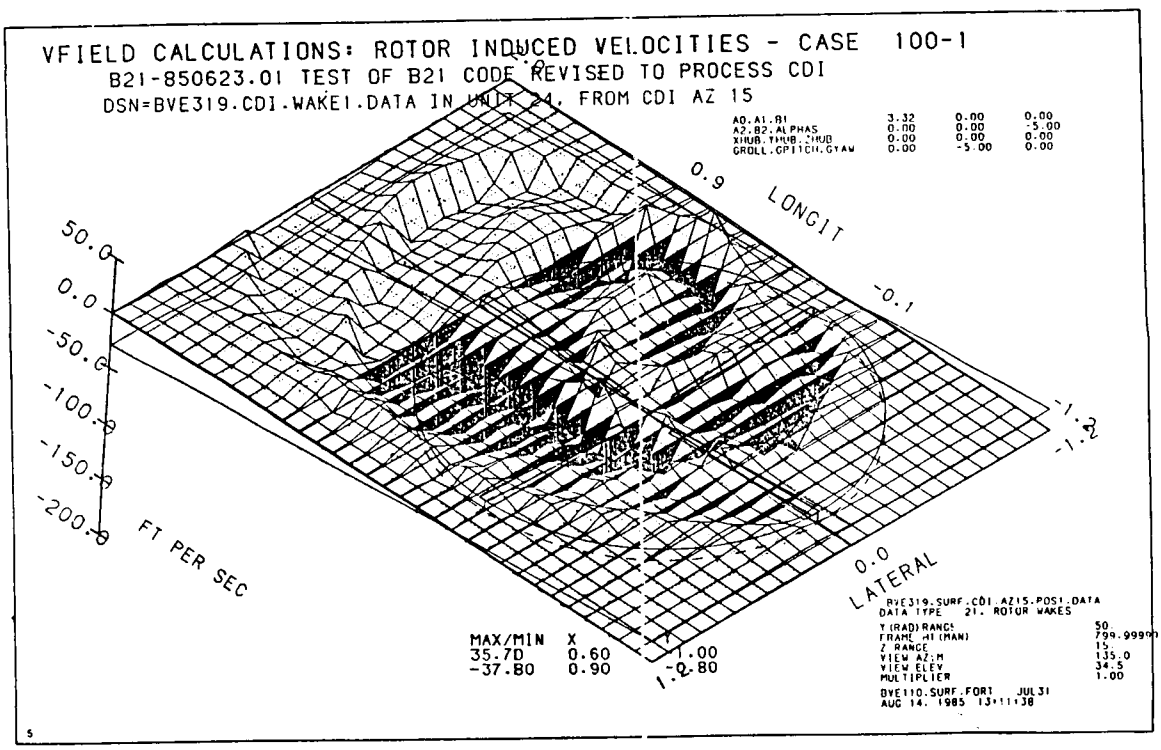

Figure 20. Velocities Induced on a Horizontal Computation Plane

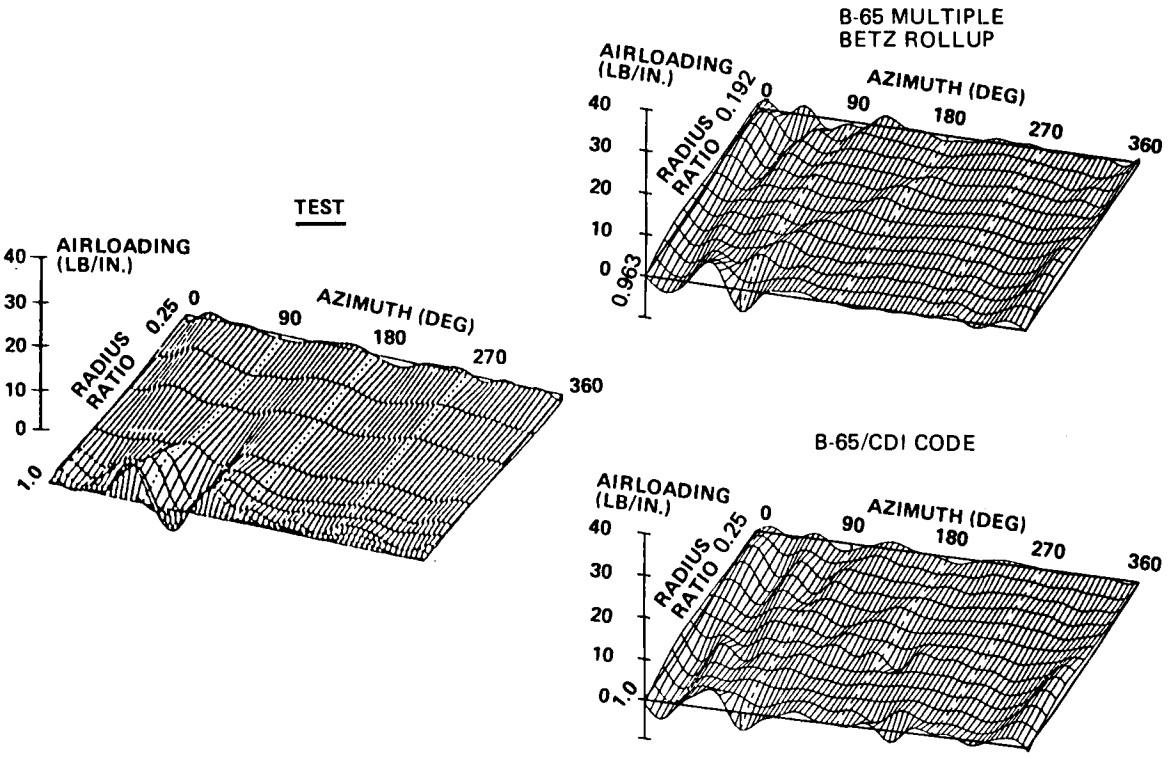

Figure 21. New Wake Models Improve Prediction of Vibratory Airloads

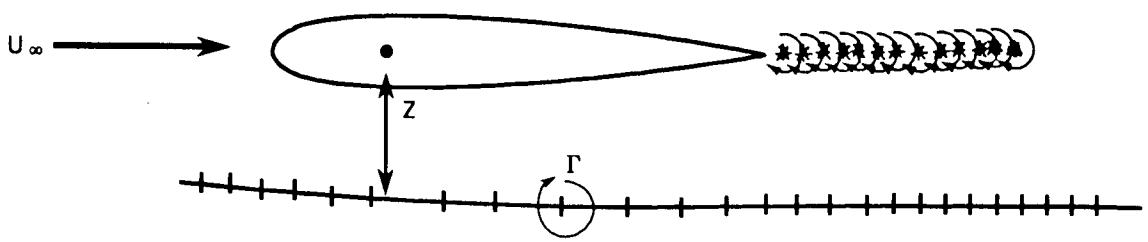

z > chord

- Lifting line valid
- Kinematic wakes useful
- Weak local 3D effects
- Wakes must have correct vorticity distribution
- Important for vibratory airloads
- Transonic CFD codes

z < chord

- Lifting line marginal
- Free wakes needed
- Moderate local 3D effects
- Approximation of BVI possible
- Important for noise and vibration
- Euler codes under development

Blade/Vortex Encounter
z = 0

- Lifting line useless
- Local 3D methods and free wakes
- Strong local 3D effects
- Accurate BVI needed
- Critical to noise reduction
- Viscosity effects

Figure 22. Illustration of BVI Regimes

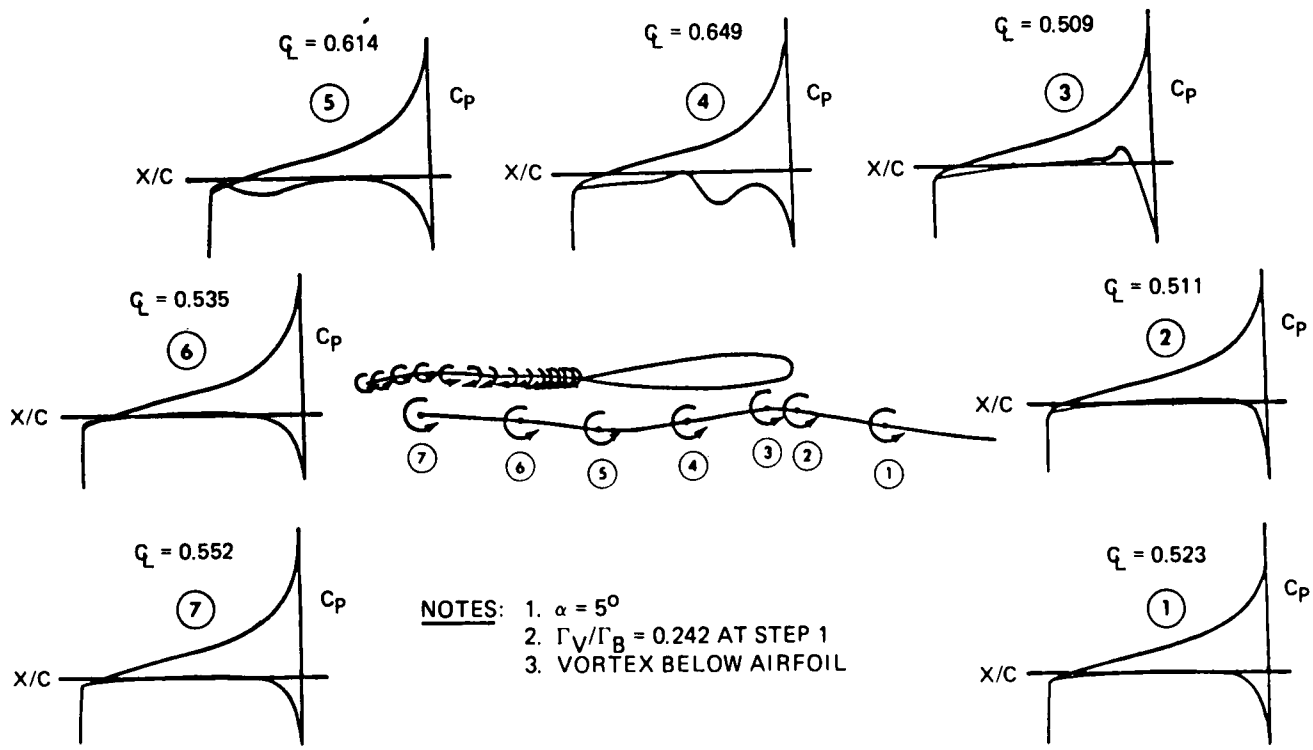

Figure 23. Effect of Blade Vortex Interaction on Instantaneous Pressure Distribution Evaluated by Joukowsky Transformation Method

LIFTING LINE VERSUS EXACT SOLUTION

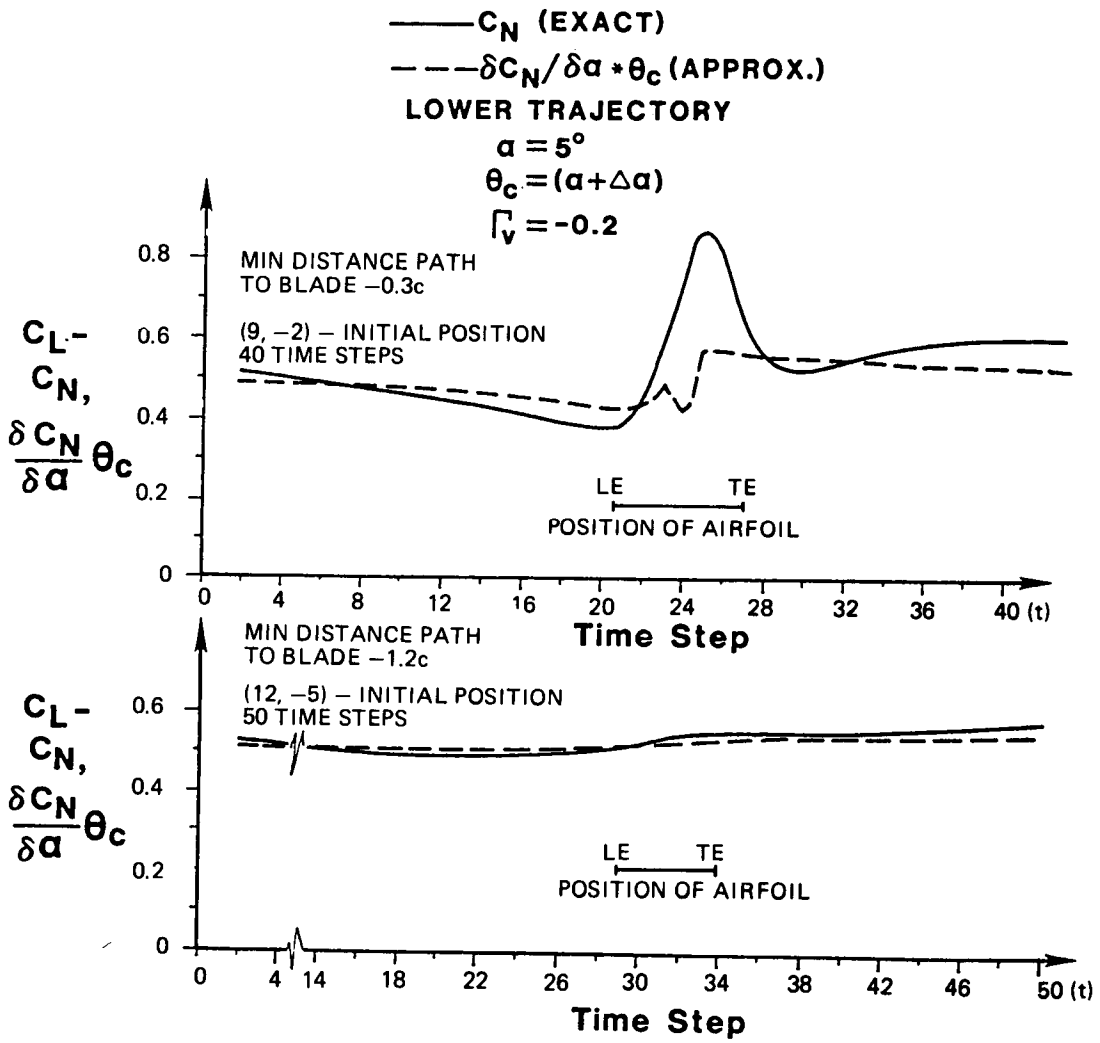

Figure 24. BVI Effects Estimated by Joukowsky Method

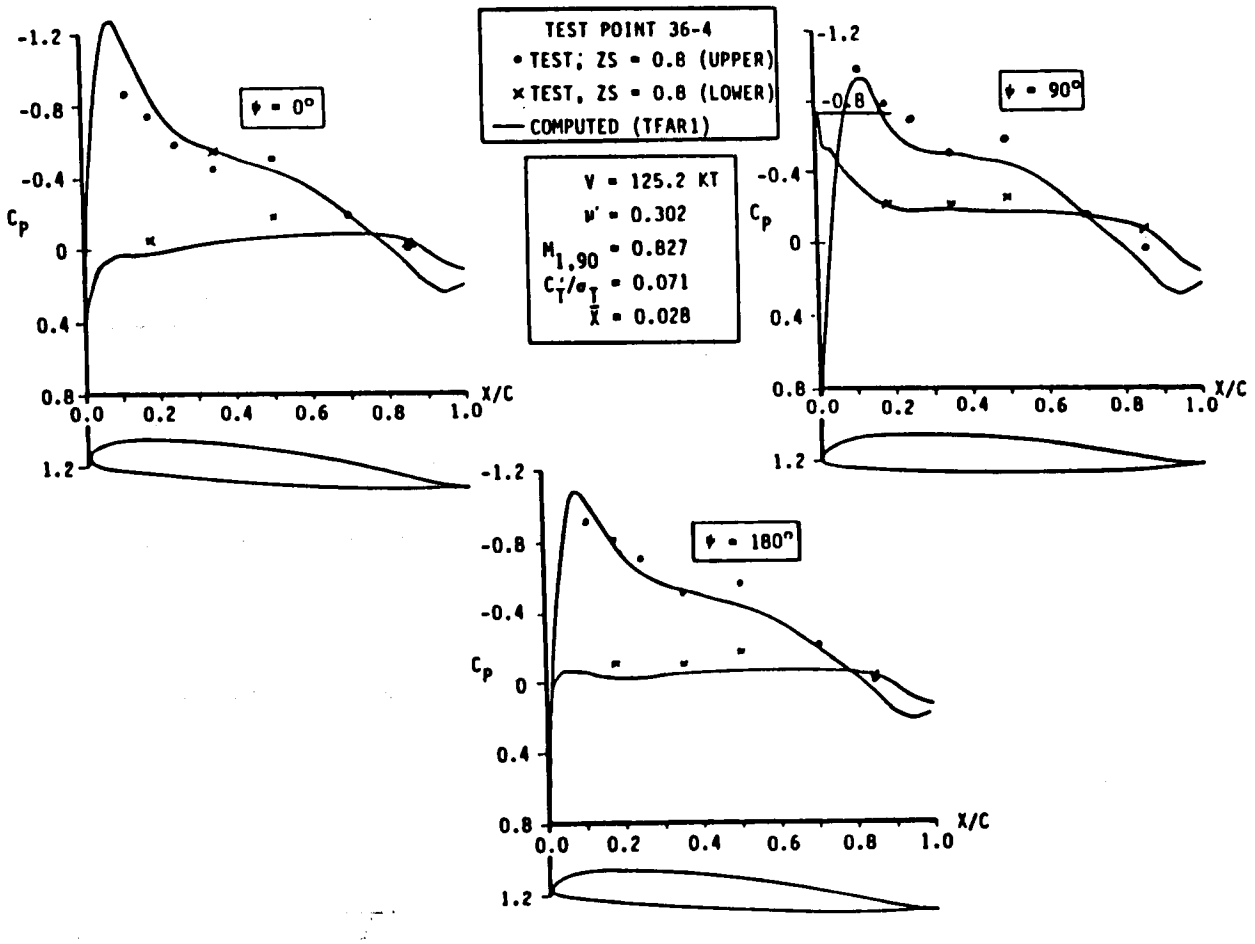

Figure 25. Test/Theory Correlation of BVWT 313 with B-65/TFAR-1

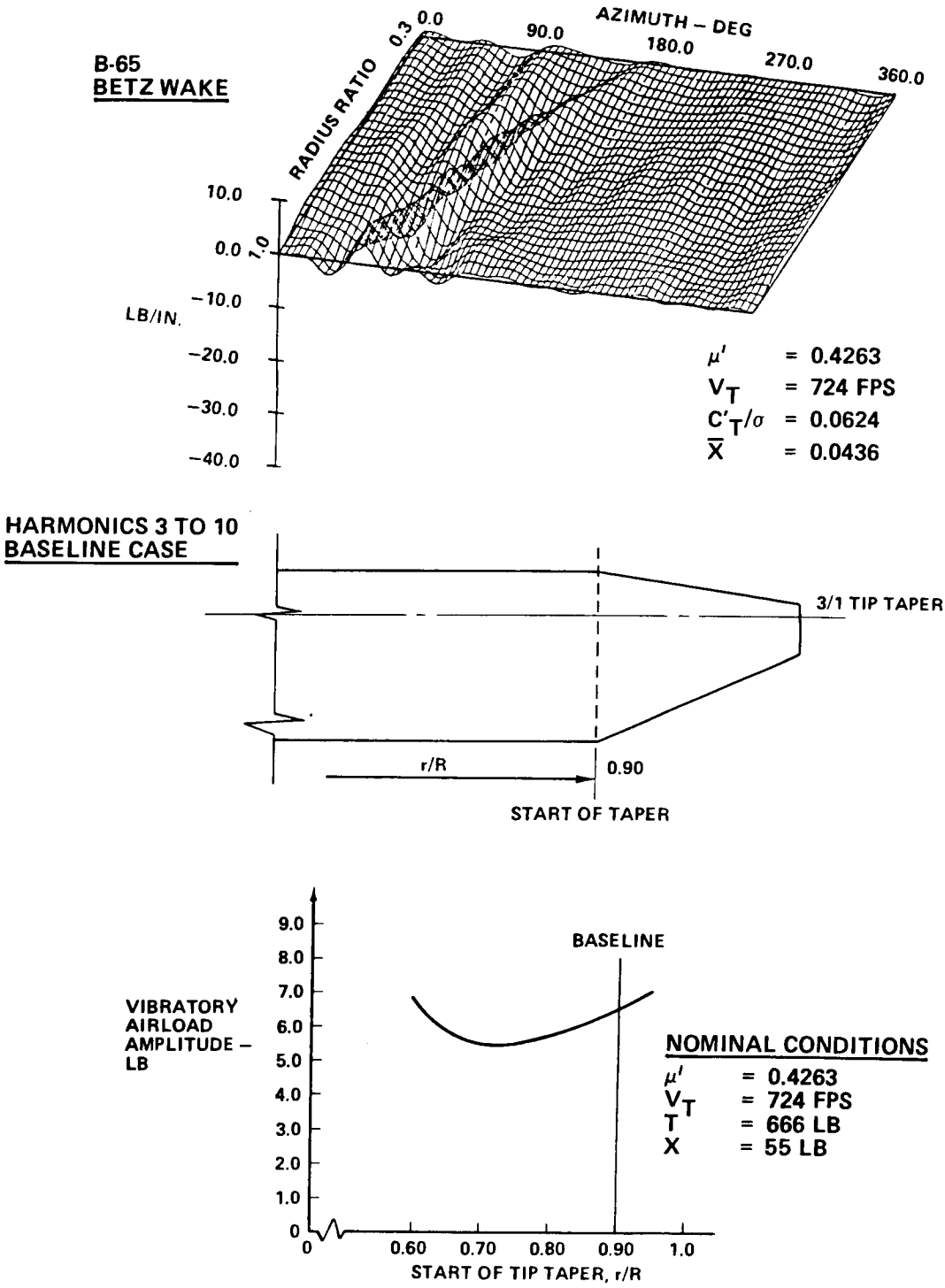

Figure 26. Vibration Reduction Trends

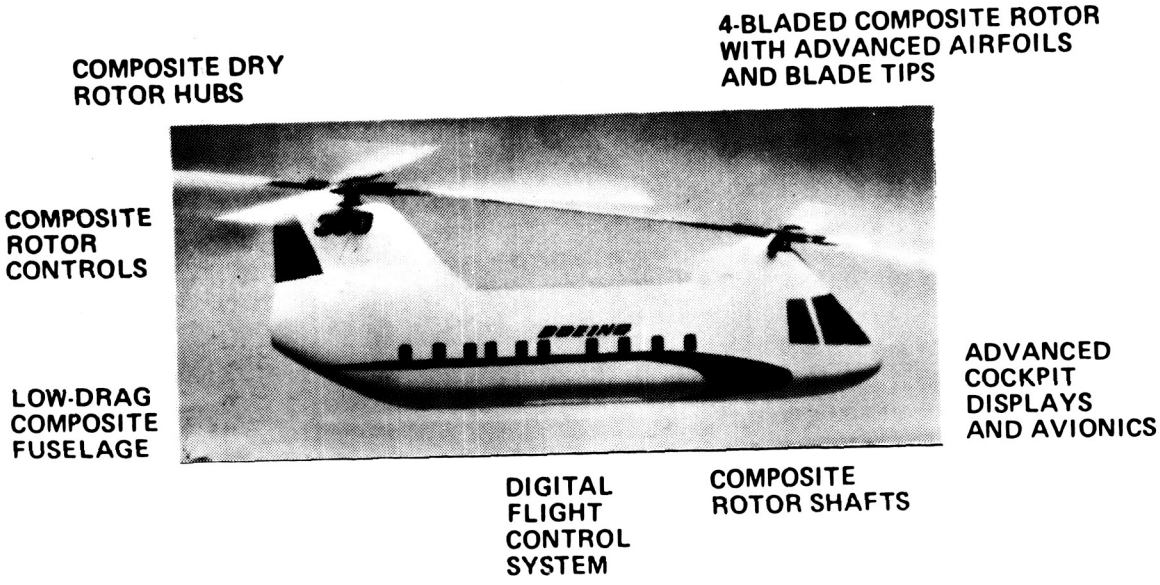

Figure 27. Model 360 Advanced Technology Helicopter

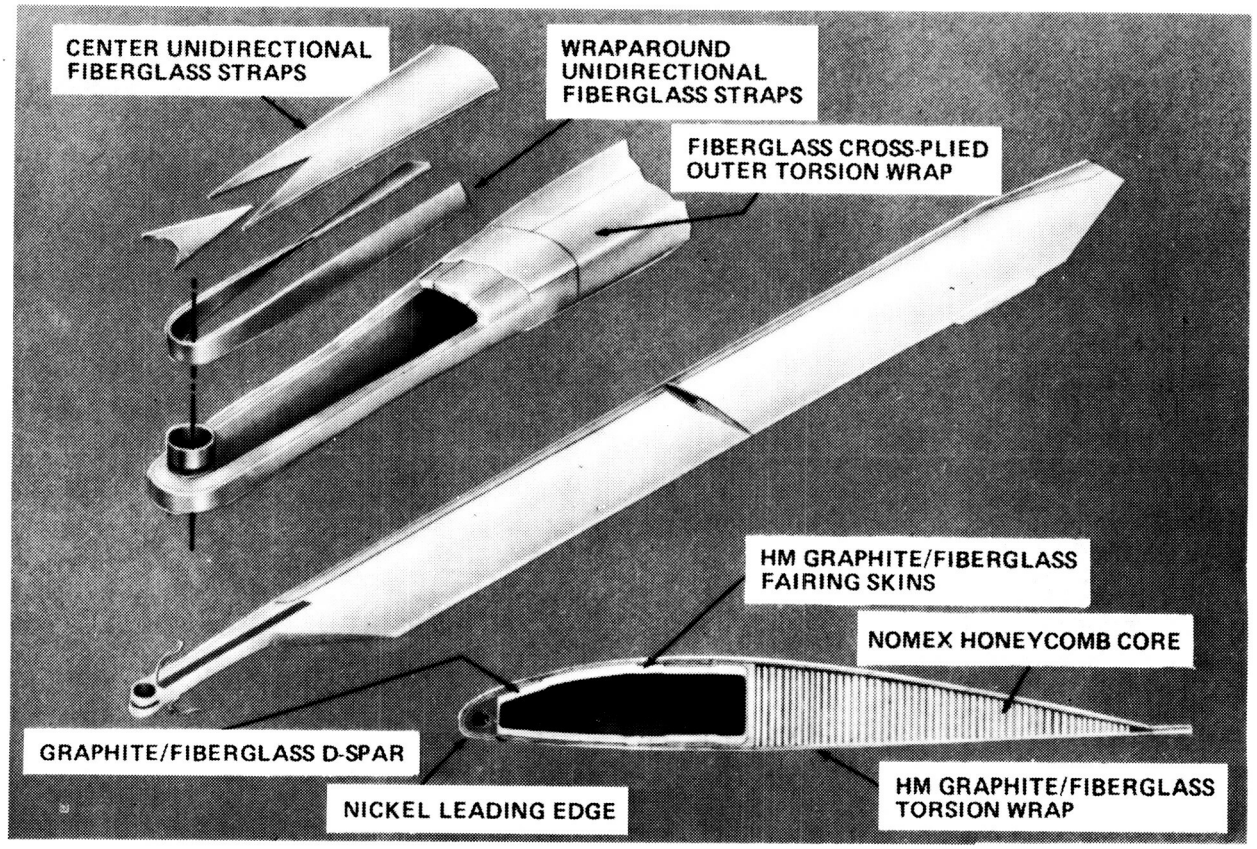

Figure 28. Model 360 High-Performance Rotor Construction (VR-12/VR-15 Airfoils)

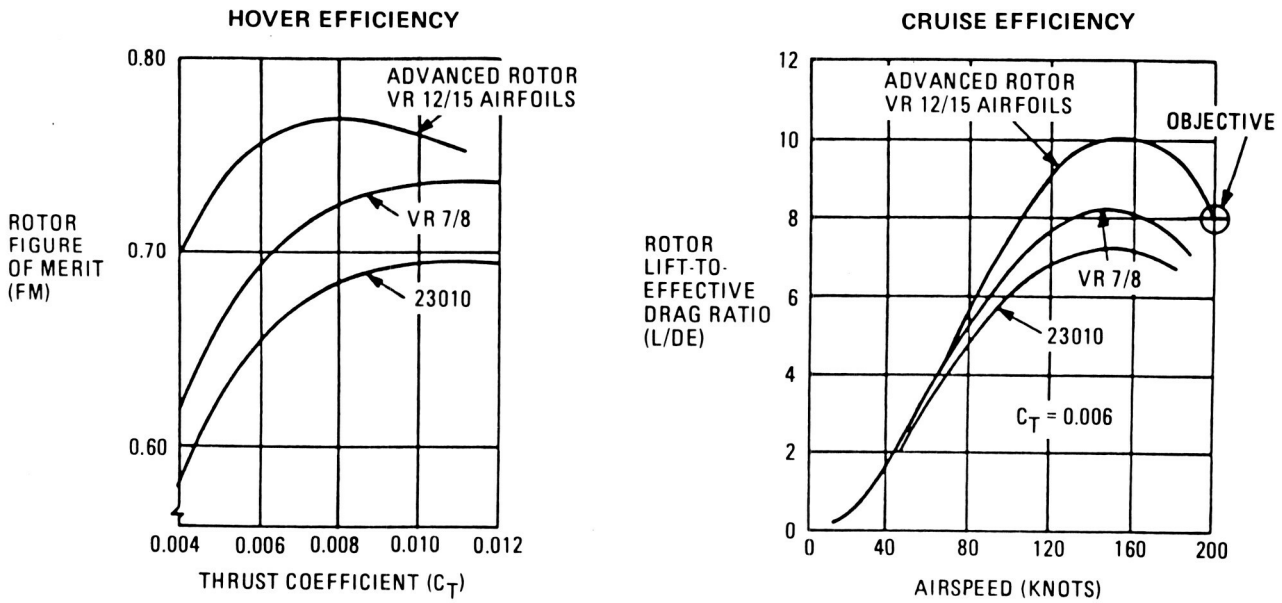

Figure 29. Model 360 High-Performance Rotor Wind Tunnel Results

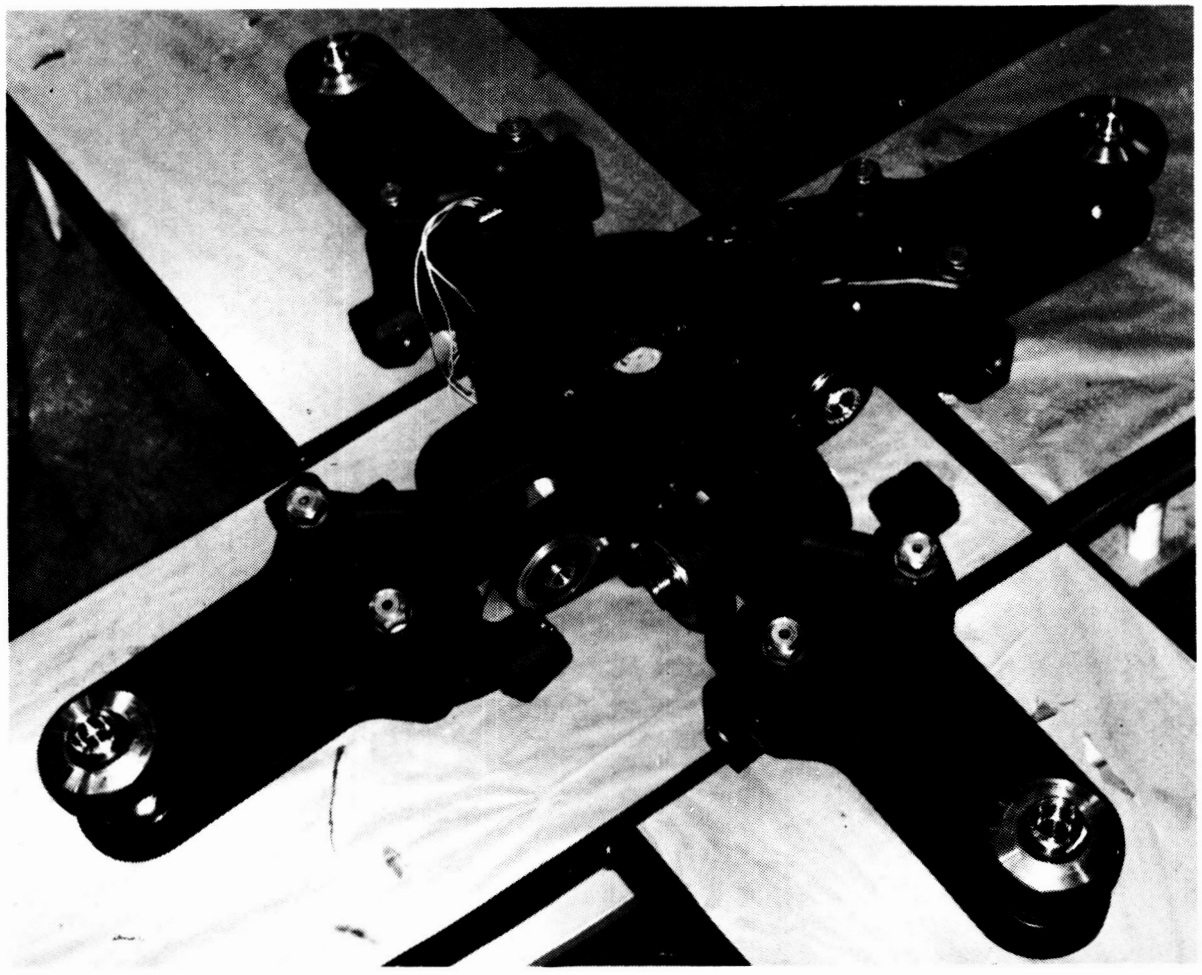

Figure 30. Model 360 Composite Dry Hub

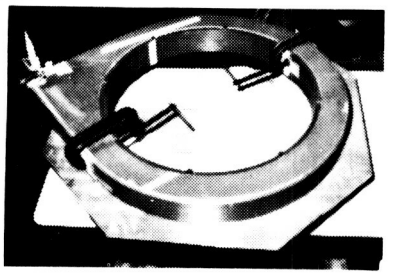

Swashplate Ring

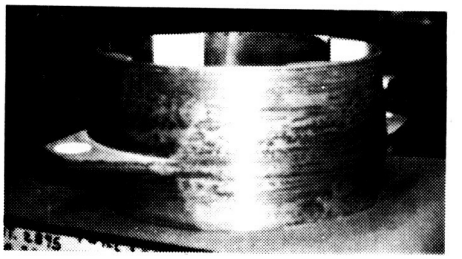

Slider

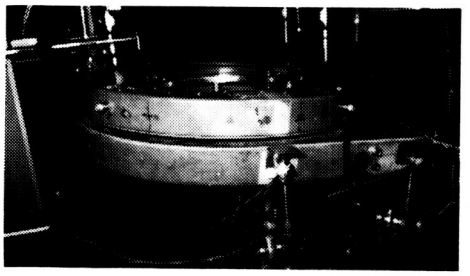

Swashplate Assembly

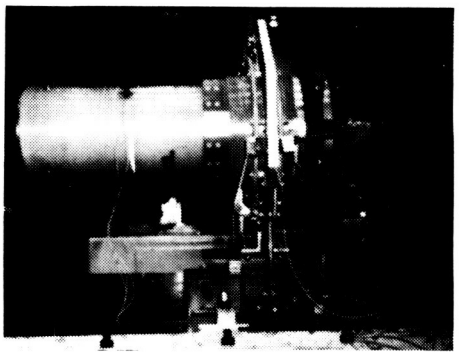

Slider Guide Assembly

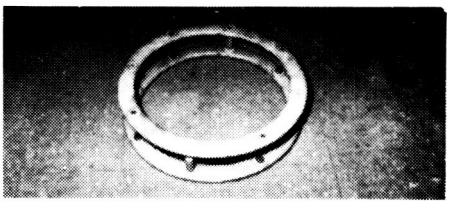

Gimbal Ring

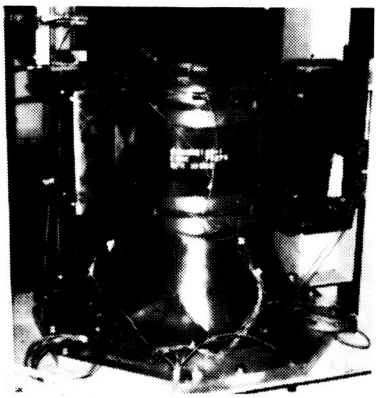

Standpipe-Actuator Supports

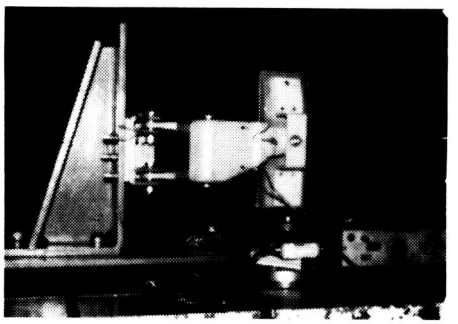

Scissors

Figure 31. Model 360 Composite Rotor Controls

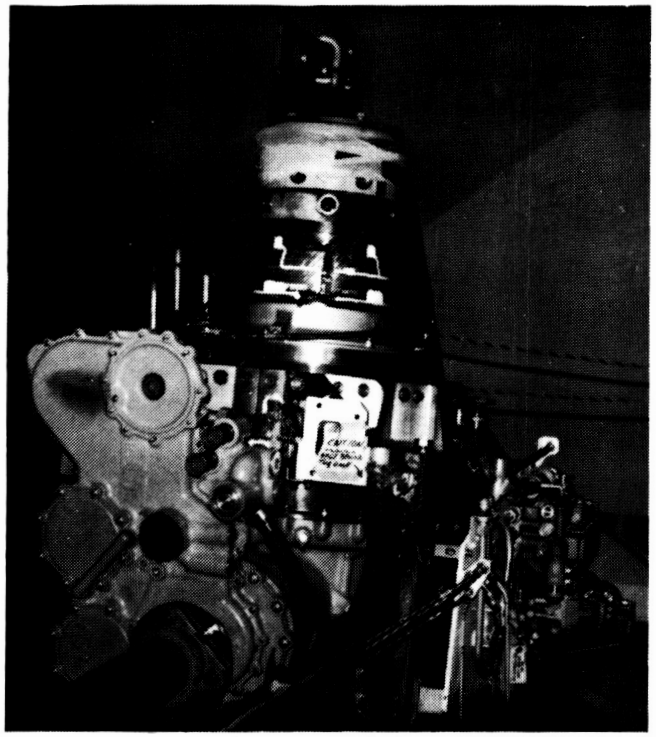

Forward Transmission

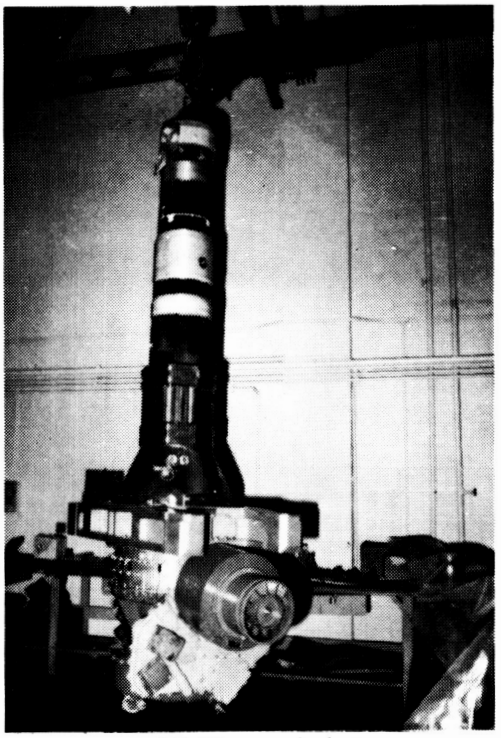

Aft Transmission

Figure 32. Model 360 Drive System: Composite Rotor Shafts

Forward Transmission Cover

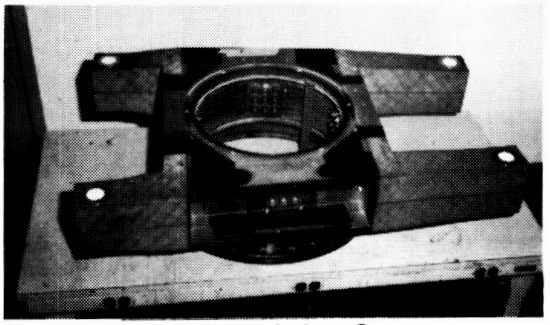

Aft Transmission Cover

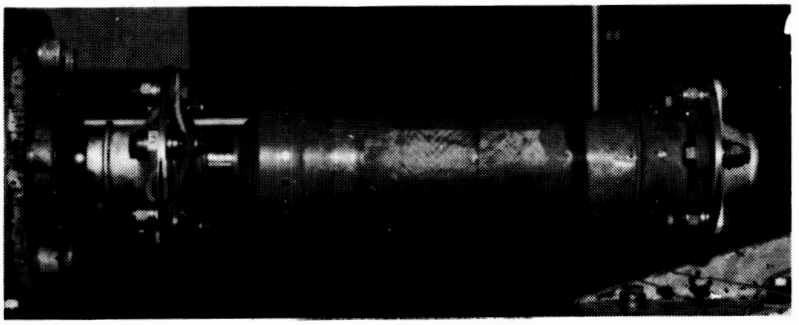

Synchronizing Shaft

Figure 33. Model 360 Drive System: Composite Components

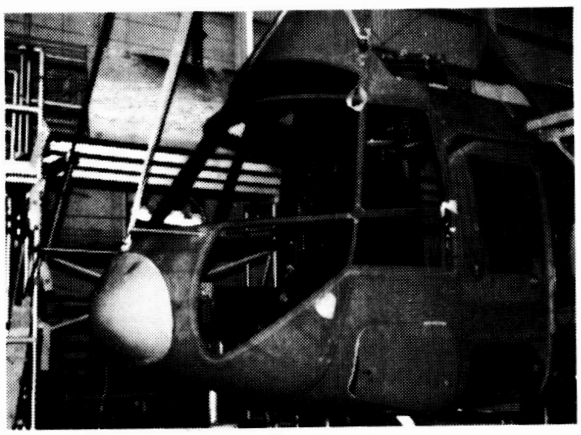

Nose Enclosure

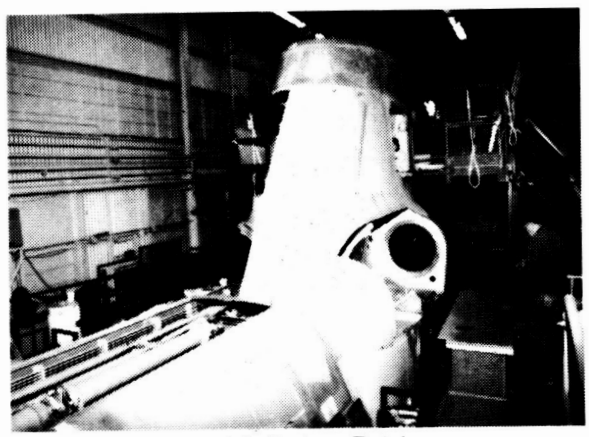

Aft Pylon Fairings

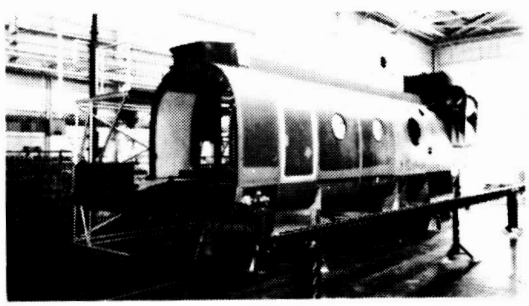

Primary Structure

Figure 34. Model 360 Composite Fuselage

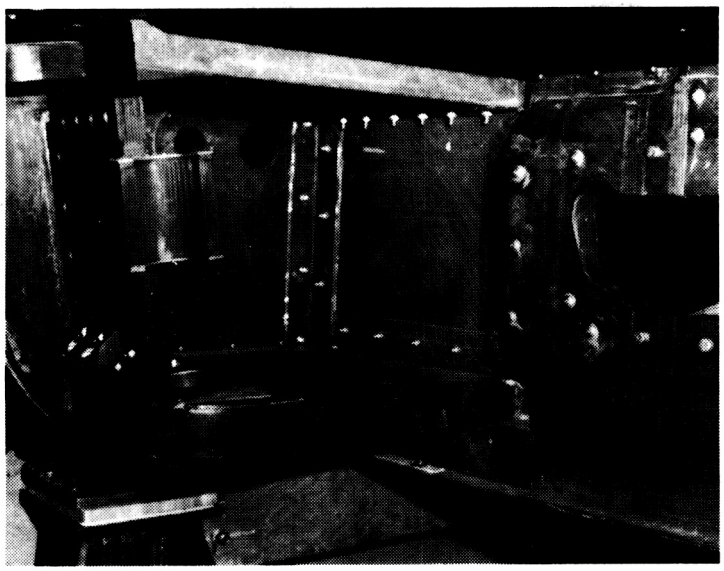

Main Landing Gear

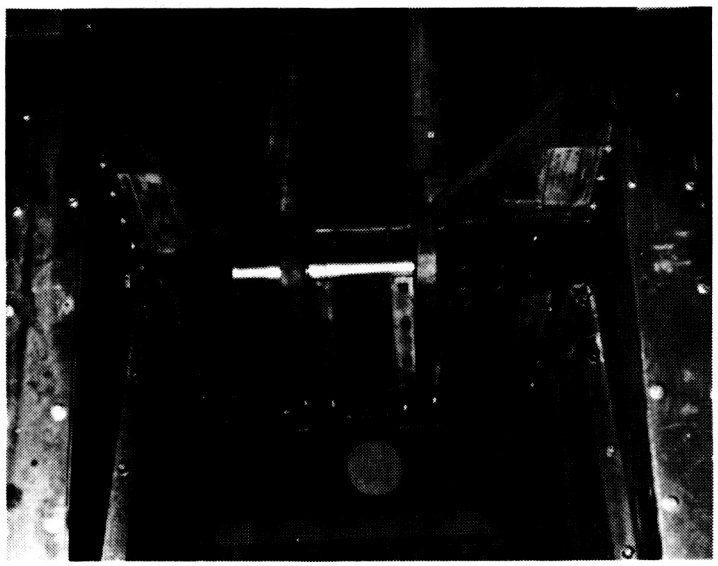

Nose Gear

Figure 35. Model 360 Fuselage Composite Backup Structure

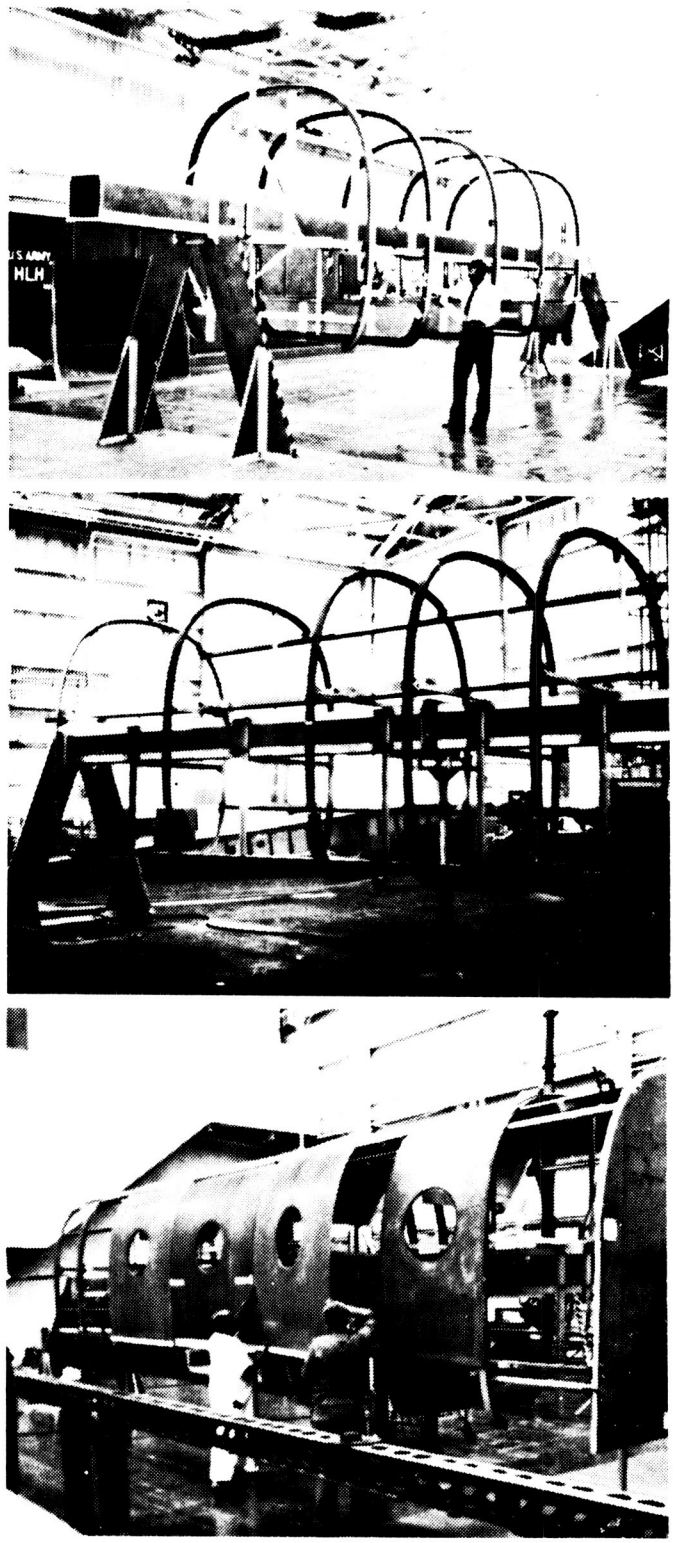

Figure 36. Model 360 Composite Fuselage Assembly

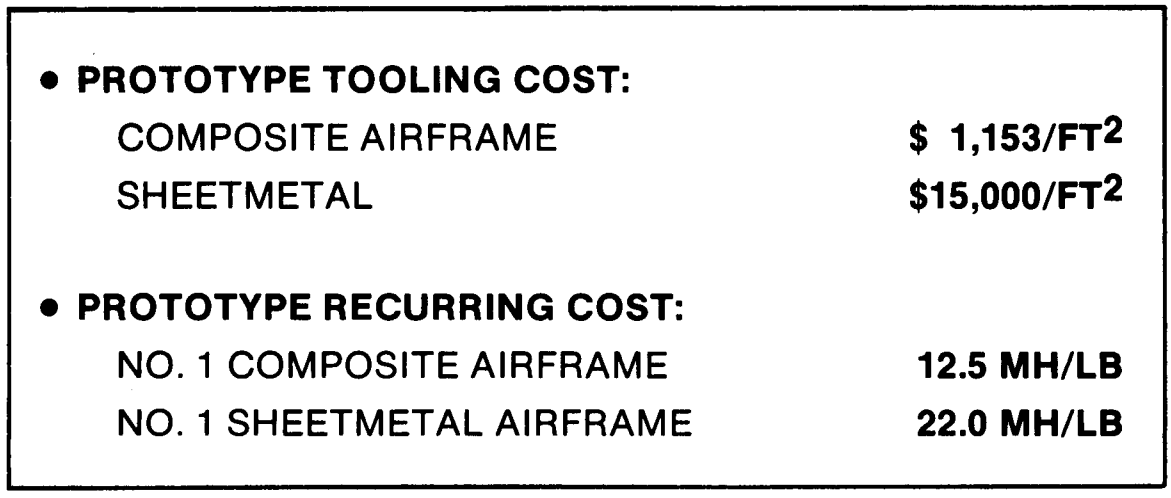

Figure 37. Cost Experience with Advanced Composite Airframe

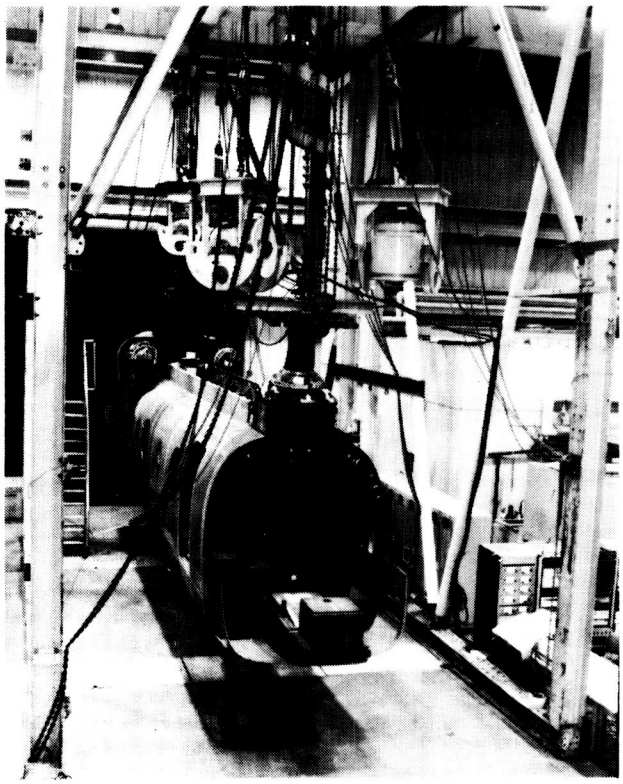

Shake

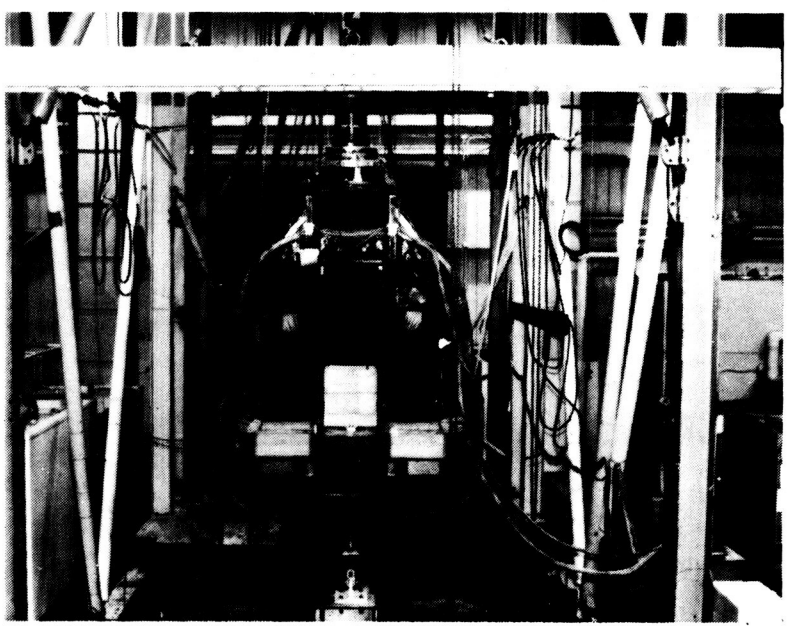

Static Load

Figure 38. Model 360 Composite Fuselage Development Tests

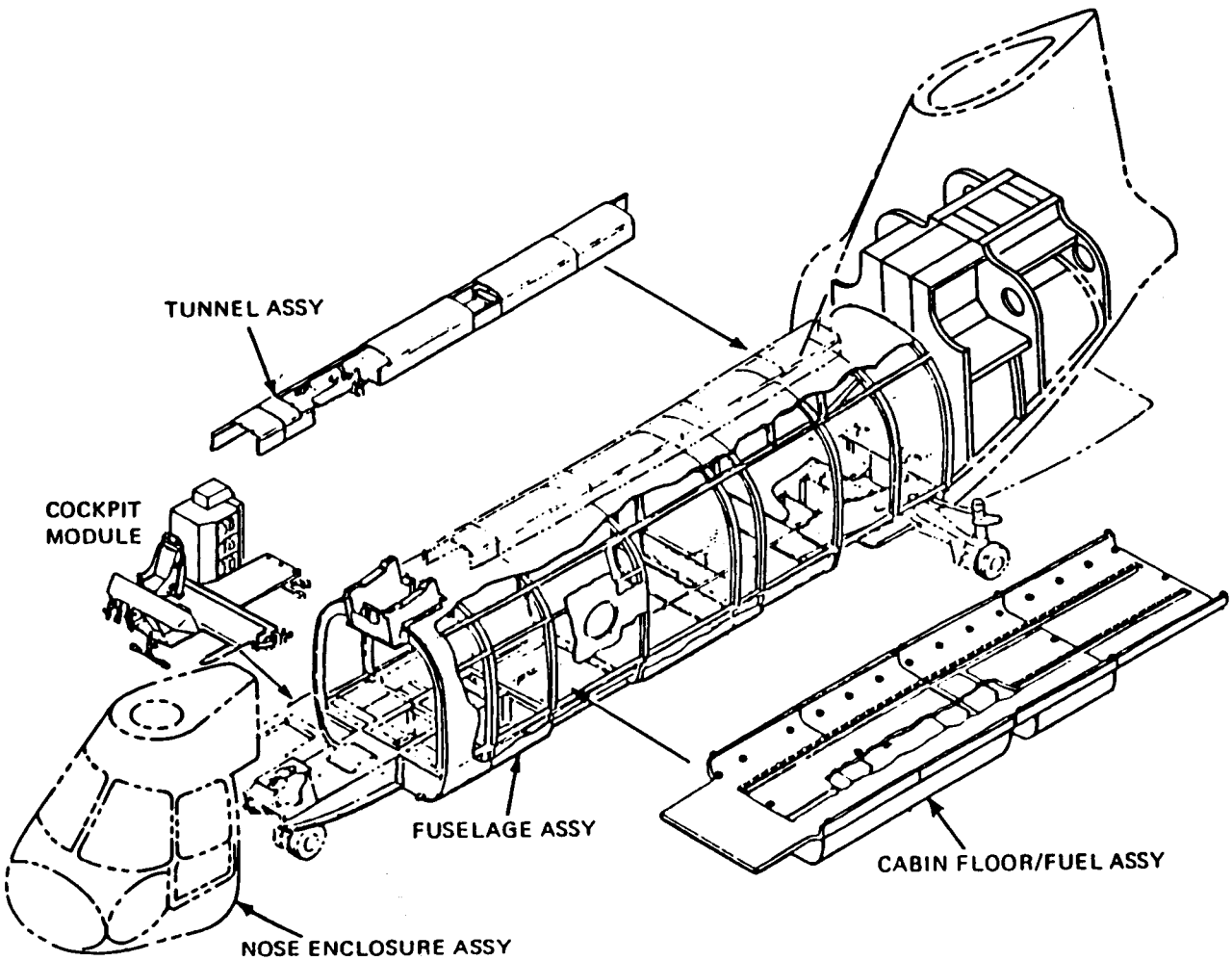

Figure 39. Model 360 Fuselage and Subsystem Modules

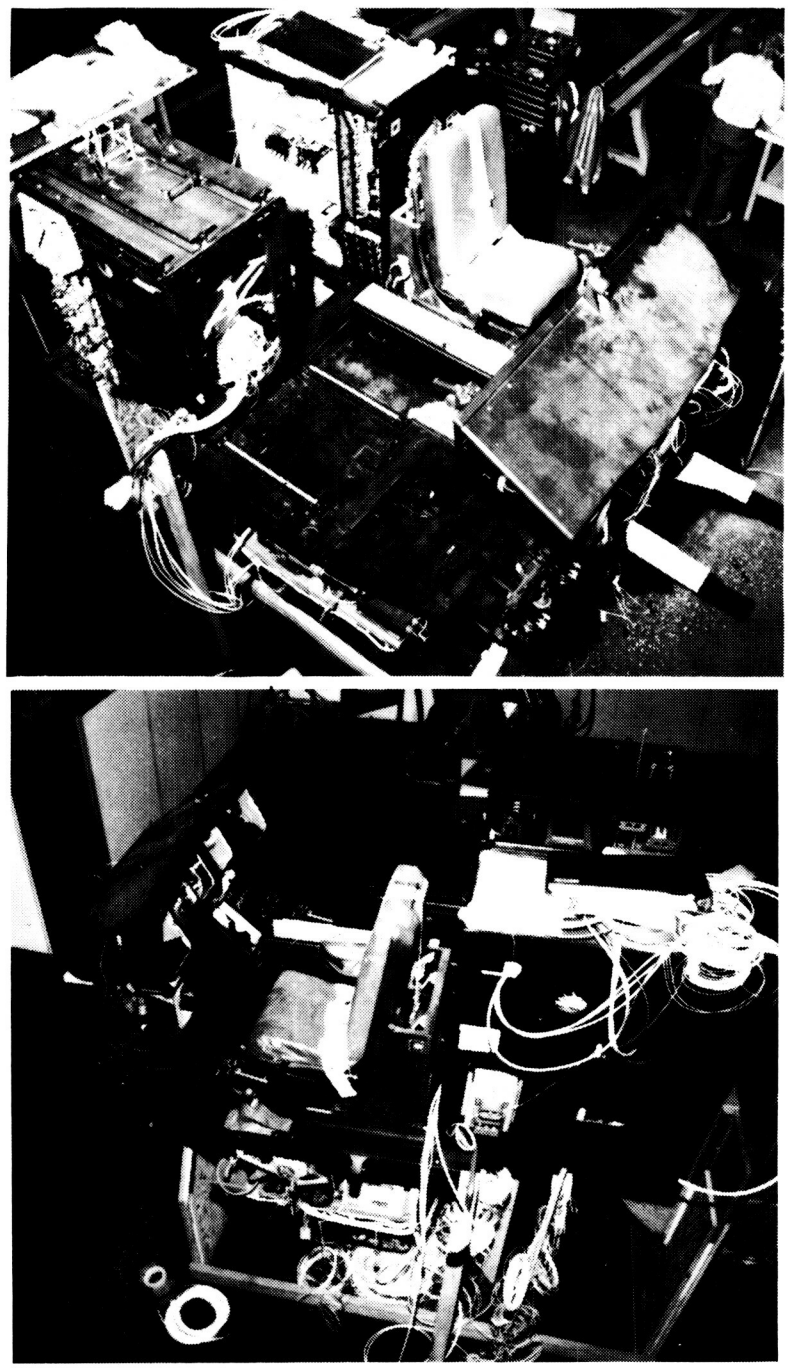

Figure 40. Model 360 Cockpit Module Assembly

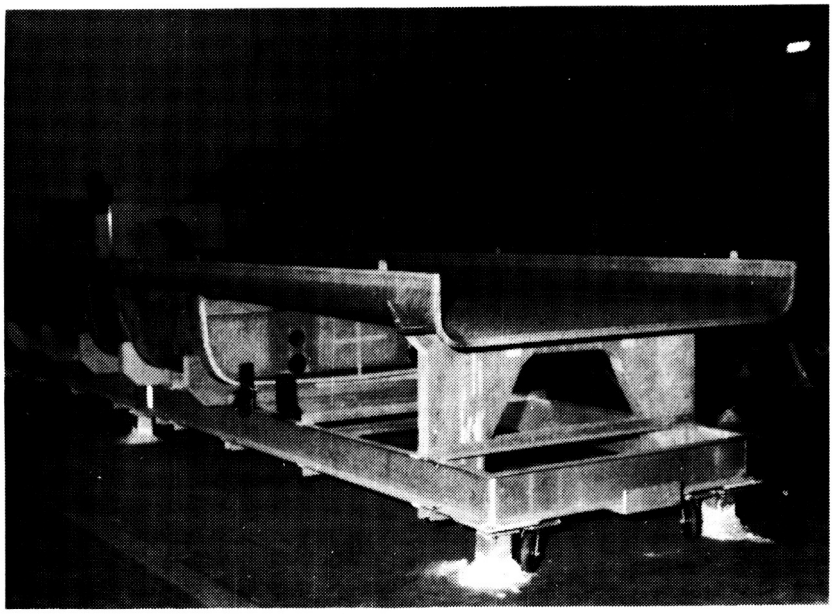

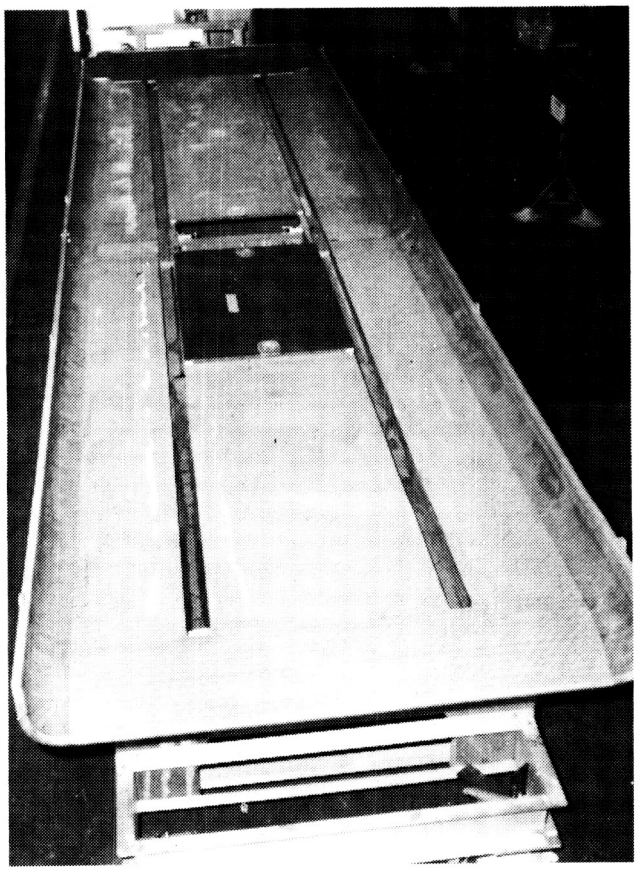

Figure 41. Model 360 Composite Floor Module

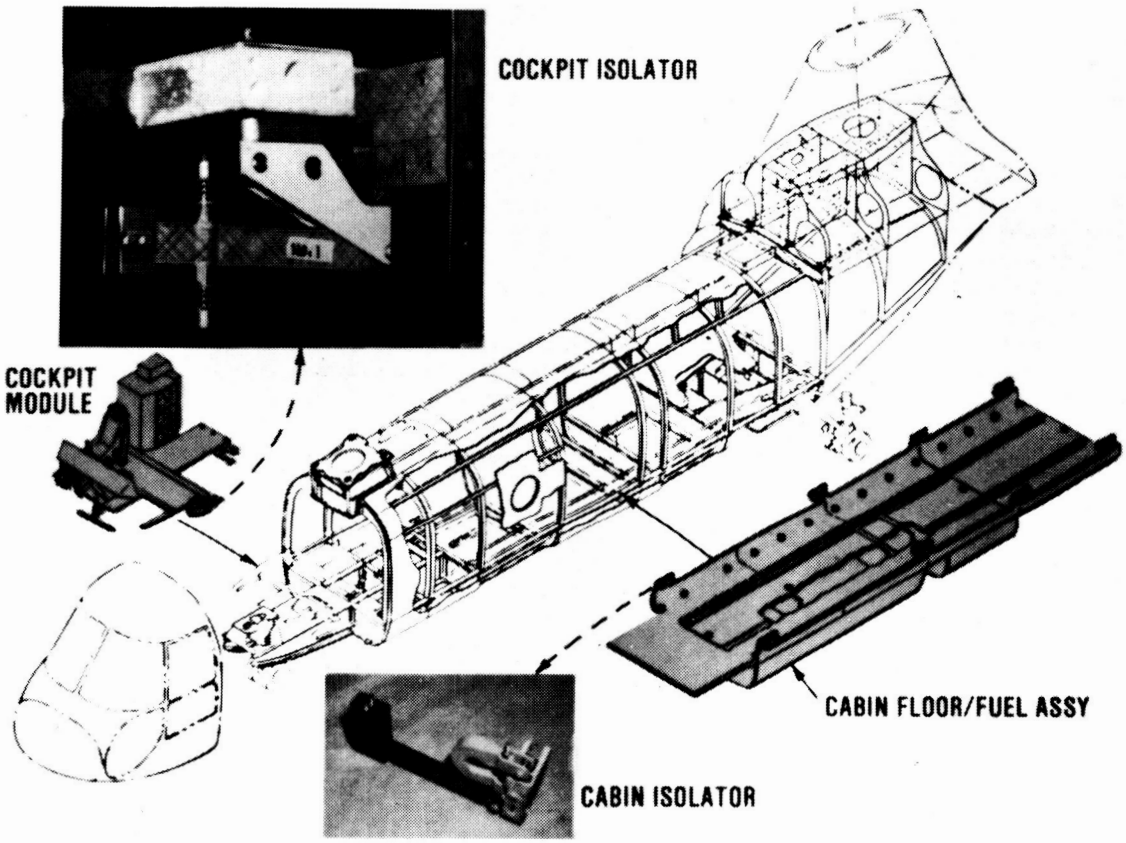

Figure 42. Model 360 Vibration-Isolated Modules

- Modularized Hydraulics

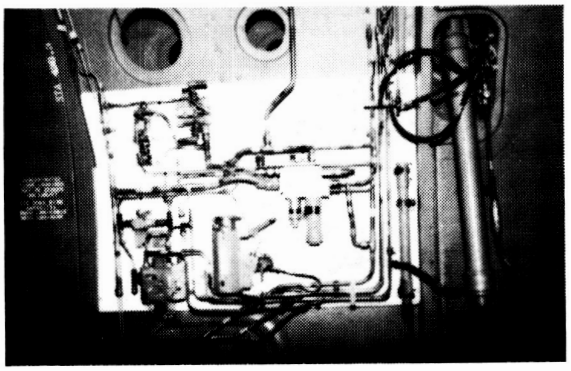

- Digital AFCS
- Integrated Avionics System

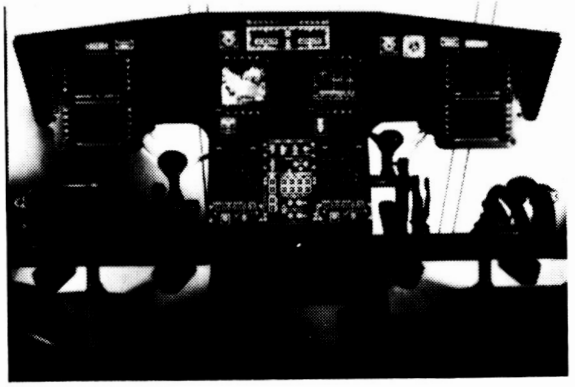

- Composite Landing Gear Components

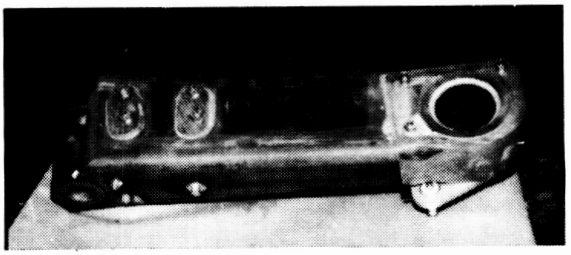

Figure 43. Model 360 Advanced Subsystems

	V-22	CH-47 GROWTH	LHX
COMPOSITE STRUCTURES			
— DEMONSTRATE TOOLING CONCEPTS	X	X	X
— DEMONSTRATE EFFICIENT DESIGNS	X	X	X
— DEVELOP DIRECTLY APPLICABLE:			
TOOLS		X	
FLIGHT HARDWARE		X	
— DEVELOP EFFICIENT SUBSYSTEM INTEGRATION CONCEPTS	X	X	X
ADVANCED ROTOR SYSTEM			
— HIGH-SPEED FLIGHT, 200 KNOTS		X	X

Figure 44. Model 360 Aerodynamic and Material Research Supports Boeing Programs